EUROPEAN Journal of Molecular Biotechnology

Has been issued since 2013.
ISSN 2310-6255. E-ISSN 2409-1332
2015. Vol.(10). Is. 4. Issued 4 times a year

The journal is registered by Federal Service for Supervision of Mass Media, Communications and Protection of Cultural Heritage (Russia). Registration Certificate **ПИ № ФС77-55114** 26.08.2013.

Journal is indexed by: **Chemical Abstracts Service** (USA), **CiteFactor** – Directory of International Reseach Journals (Canada), **Cross Ref** (UK), **EBSCOhost Electronic Journals Service** (USA), **Global Impact Factor** (Australia), **International Society of Universal Research in Sciences** (Pakistan), **Journal Index** (USA), **Electronic scientific library** (Russian Federation), **Open Academic Journals Index** (Russian Federation), **Sherpa Romeo** (Spain), **ULRICH's WEB** (USA), **Universal Impact Factor** (Australia).

All manuscripts are peer reviewed by experts in the respective field. Authors of the manuscripts bear responsibility for their content, credibility and reliability.

Editorial board doesn't expect the manuscripts' authors to always agree with its opinion.

Postal Address: 26/2 Konstitutcii, Office 6
354000 Sochi, Russian Federation

Website: http://ejournal8.com/
E-mail: ejm2013@mail.ru

Founder and Editor: Academic Publishing House *Researcher*

Passed for printing 16.12.15.
Format 21 × 29,7/4.
Enamel-paper. Print screen.
Headset Georgia.
Ych. Izd. l. 4,5. Ysl. pech. l. 4,2.

Order № 10.

European Journal of Molecular Biotechnology

2015

Is. 4

Европейский журнал молекулярных биотехнологий

2015

№ 4

Европейский журнал молекулярных биотехнологий

Издается с 2013 г. ISSN 2310-6255. E-ISSN 2409-1332
2015. № 4 (10). Выходит 4 раза в год.

Журнал зарегистрирован Федеральной службой по надзору в сфере массовых коммуникаций, связи и охраны культурного наследия (Российская Федерация). Свидетельство о регистрации средства массовой информации ПИ № ФС77-55114 от 26.08.2013 г.

Журнал индексируется в: **Chemical Abstracts Service** (США), **CiteFactor** – Directory of International Reseach Journals (Канада), **Cross Ref** (Великобритания), **EBSCOhost Electronic Journals Service** (США), **Global Impact Factor** (Австралия), **International Society of Universal Research in Sciences** (Пакистан), **Journal Index** (США), **Научная электронная библиотека** (Россия), **Open Academic Journals Index** (Россия), **Sherpa Romeo** (Испания), **ULRICH's WEB** (США), **Universal Impact Factor** (Австралия).

Статьи, поступившие в редакцию, рецензируются. За достоверность сведений, изложенных в статьях, ответственность несут авторы публикаций.
Мнение редакции может не совпадать с мнением авторов материалов.

Адрес редакции: 354000, Российская Федерация, г. Сочи, ул. Конституции, д. 26/2, оф. 6
Сайт журнала: http://ejournal8.com/
E-mail: ejm2013@mail.ru

Учредитель и издатель: ООО «Научный издательский дом "Исследователь"» - Academic Publishing House *Researcher*

Подписано в печать 16.12.15.
Формат 21 × 29,7/4.
Бумага офсетная.

Печать трафаретная.
Гарнитура Georgia.
Уч.-изд. л. 4,5. Усл. печ. л. 4,2.
Заказ № 10.

CONTENTS

Published in the Russian Federation
European Journal of Molecular Biotechnology
Has been issued since 2013.
ISSN: 2310-6255
E-ISSN: 2409-1332
Vol. 10, Is. 4, pp. 188-196, 2015

DOI: 10.13187/ejmb.2015.10.188
www.ejournal8.com

UDC 546.05:546.47:546.06

The Effect of Titanium Dioxide Nanoparticles on Salivary Alkaline Phosphatase Activity

[1] Eaman A. S. AL-Rubaee
[2] Suha T. Abd
[3] Nadia M. Kadim

[1] University of Baghdad, Iraq
Assistant Professor, Department of Basic Sciences
College of Dentistry
[2] University of Baghdad, Iraq
Assistant Lecturer, Department of Basic Sciences
College of Dentistry
[3] University of Baghdad, Iraq
Assistant Lecturer, Department of Periodontology
College of Dentistry

Abstract

The structural and optical properties of the titanium dioxide nanoparticles [TiO2 NPs] have been investigated using [UV-Vis] spectrophotometer and SEM. The produced nanoparticles show small and about sharp round peaks around 220 nm. The produced nanoparticles have a spherical shape with an average particle size <50 nm. The effect of titanium dioxide NPs was studied on the activity of Alkaline Phosphatase [ALP] in the saliva of 25 patients with gingivitis in comparison to 20 healthy subjects with the average age about 22–23 years for both groups. The results correlated with the observation that salivary alkaline phosphatase activity increase in patient with gingivitis in comparison to control group and salivary ALP activity inhibited by titanium dioxide nanoparticles.

Keywords: TiO2 nanoparticles, ALP activity, gingivitis, saliva.

Introduction

Periodontal diseases are bacterial infections of the gingiva, bone and attachment fibers that support the teeth and hold them in the jaw. The main cause of the diseases is a bacterial plaque, a sticky, colorless microbial film that constantly forms on teeth [1]. The microbial plaque accumulation on teeth surfaces adjacent to the gingival tissues brings the oral sulcular and junctional epithelial cells into contact with the waste product, enzymes and surface components of colonizing bacteria. As the bacterial load increases so do the irritation of the host tissues by these substances [2]. From the periodontal diseases gingivitis and periodontitis are the two predominant periodontal diseases and may be present at the same time. In gingivitis, the gingival are inflamed but their destruction is reversible while in periodontitis the inflammatory changes are irreversible changes [3]. Gingivitis represents the inflammation process limited to the gingival tissue next to the tooth without any loss of attachment and possibly acts as a precursor to attachment loss around the tooth [4]. Gingivitis is typically characterized as a vigorous inflammatory response limited

mostly to the superficial gingival connective tissues and is a comparatively nonspecific response to a nonspecific bud up of dental plaque. With continuing plaque accrual, gingivitis becomes well established, but still confined to the superficial gingival connective tissues [5].

In humans, alkaline phosphatase [ALP] exists in each tissue through the entire body, but is specially concentrated in liver, bile duct, bone, kidney, the placenta and intestinal mucosa [6]. The enzyme ALP plays a role in bone metabolism. It is a glycoprotein enzyme that is bounded to membrane and it produced by many cells, such as leukocytes, polymorphonuclear, macrophages, fibroblasts, and osteoblasts in the area of the gingival tissue and periodontium [7]. Gao J. et al. [8] show that the highest ALP activity was found in osteoblasts, but moderate in periodontal ligament PDL fibroblasts, and lowest in gingival fibroblasts. No activity was detected in cementoblasts. In the periodontium, the ALP is very important enzyme as it is part of normal turnover of periodontal ligament, root cementum and maintenance, and bone homeostasis. Some forms of enzyme are also produced by plaque bacteria [9]. Some studies have shown a strongly increased activity of salivary alkaline phosphatase in periodontal disease particularly in the acute phase, and after the periodontal rehabilitation, the activity of these enzymes restored to the normal value that found in the healthy persons [10].

Nanoparticles have many different effects on human health relative to bulk original material from which they are produced [11]. Consequently of their tiny size, nanoparticles may propose other advantages to the biomedical field through increased biocompatibility [12]. Studies of the effects of nanoparticles [NPs] from different industry branches on cells and pathways are emerging, and most of the biological effects of NPs seem to be due to their interactions with proteins [13]. Enzymes are biologic polymers that catalyze the chemical reactions that make life possible, with the exception of catalytic RNA molecules, or ribozymes, enzymes are proteins [14].

In current years, metal oxide nanoparticles have been mainly examined for their antimicrobial activity, especially titanium dioxide which is considered a clean photo catalyst, low-cost, with nontoxicity and chemical stability [15, 16]. Titanium dioxide nanoparticles are produced universally for multiplicity of engineering and bioengineering uses. Titanium dioxide nanoparticles are often consumed as a material for orthopedic implants. TiO_2 in powder form is also commonly used as a whitener in toothpastes [15, 16]. Titanium dioxide is the most extensively used white pigment because of its brilliance and refractive index for it which is very high, in which it is exceeded just by a few other materials. About 4.6 million tons of pigmentary TiO_2 are used yearly, and this number is likely to increase as application continues to rise [17].

There is no study about the effect of TiO_2 NPs on ALP activity in saliva of gingivitis patients, so we decided to investigate this effect in this research.

Material and methods

1. Nanoparticles

Titanium dioxide nanoparticles have been obtained from Hongwunanmter, China. This product supplies as TiO_2 Nano powder. Absorbance spectra of NPs solution were measured by UV-VIS spectrophotometer. All spectra were measured at room-temperature in a quartz cell with 1 cm optical path. The structure and nano size measurement of nanoparticles samples were identified by the Scanning Electron Microscope SEM (Electronic Microscope Centre-Collage of applied Science, University of Technology, Iraq).

2. Salivary Alkaline Phosphatase assay

Alkaline phosphatase activity was measured to determine the best saliva volume for this experiment by using different volume of sample 20, 40, 60, 80 and 100 µl. The salivary Alkaline Phosphatase activity was determined spectrophotometrically according to the recommendation of the German Clinical Chemistry Association using the kit of Human Company, Germany. The reaction mixture contained a substrate 50 mmol/L p-Nitrophenylphosphate, and a buffer contained 1.25 mol/L Diethanolamine buffer [pH 10.35±0.2] and 0.625 mmol/L magnesium chloride in a total volume of 1.250 ml. In the presence of alkaline phosphatase [100 µL of saliva], p-nitrophenylephosphate is reduced to p-nitrophenol. The rate of decrease in absorbance at 405 nm is directly proportionate to the ALP activity in the sample.

3. Collection of Saliva

Unstimulated saliva of 25 patients with gingivitis from teaching hospital of College of Dentistry/University of Baghdad was collected. The diagnosis of the patients was done by the

following assessment parameters: Gingival index [Loe and Sillness] [18], and Plaque index [Sillness and Loe] [19]. Another 20 healthy samples were collected from dental students with average age about 22-23 years for both groups. Collection was performed during 2-3 hours after the volunteer usual breakfast time and after thoroughly rinsing the mouth with water. Saliva was collected by standard spitting method from both groups: control and gingivitis group then saliva collected in a plane tube, centrifuged 10 min at 1500 g, and the supernatant liquid was used for chemical analysis.

4. Effect of TiO2 nanoparticles on salivary ALP activity

Stock solution of [200 µg/ml] concentration of TiO2 NPs was prepared and then the following concentrations 10, 20, 30, 50, and 100 µg\ml are prepared by diluting with the same solvent. The enzyme ALP activity was measured in human saliva by using 100 µl of saliva in the same method with replace 20 µl of the solvent [3:1,water:ethanol] with 20 µl of TiO2 NPs solution. The percentage effect on activity was calculated by comparing the activity with and without the TiO2 NPs and under the same conditions according to the following equations:

% inhibition = 100 – 100 × [Activity in the presence of nanoparticles/Activity without the nanoparticles]

A constant final concentration of TiO2 NPs [0.15 µg/ml] was used to measure the enzyme activity in saliva samples of gingivitis patients and control persons.

5. Statistical analysis

Statistical analysis was performed using SPSS [version 14] and Microsoft Office Excel [Microsoft Office Excel for windows; 2010]. Data were analyzed by using Two Way Analysis of Variance [ANOVA]. The Student t-test was used to assess significant difference among means at level [$P < 0.05$].

Results and discussion

Table 1 shows the obvious difference between control group and persons with gingivitis in gingival and plaque index.

Table 1. Summary of GI and PI Scores

	N	Gingival Index [Mean ± SD]	Plaque Index [Mean ± SD]
Control persons	20	0.95±0.20	0.61±0.27
Patient with Gingivitis	25	1.37 ± 0.31	1.59 ± 0.36

Figure 1 shows the difference in mean and standard deviation for plaque index and gingival index in healthy control person [PLI, GI] and patient with gingivitis [PLI2, GI2]. The increase in the two main parameters considers from the main causes of gingivitis and this is proved in many studies.

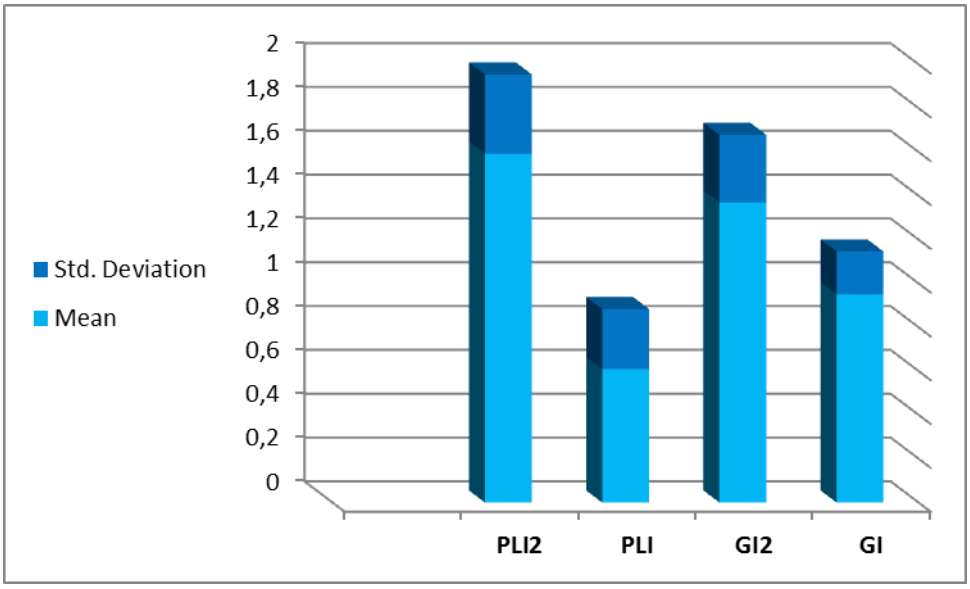

Figure 1. The difference between control in plaque index [PLI] and gingival index [GI] and gingivitis group [PLI2, GI2]

Figure 2 shows the UV-VIS absorption spectra that indicated the characteristic absorbance feature of titanium dioxide nanoparticles, illustrates absorption spectra of titanium dioxide nanoparticles, so the surface related peak could be clearly distinguished. This peak was around 240 nm. This result is in agreeement with that of Chen et al [20], which indicate the absorbance intensity of GalA-TiO2 NPs dispersion in the UV region at <300 nm.

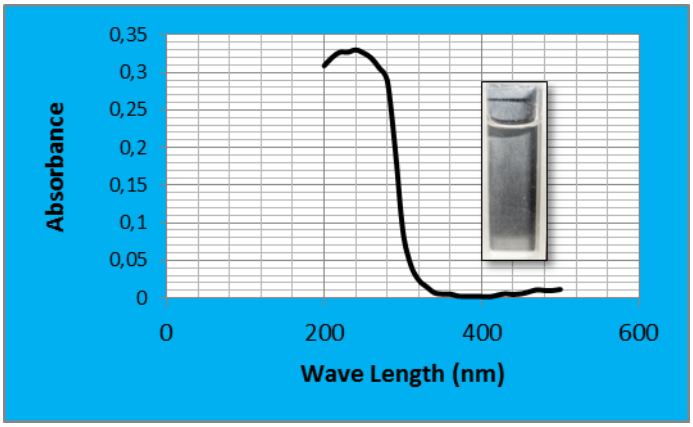

Figure 2. Absorbance spectra of the titanium dioxide nanoparticles

Figure 3 shows SEM pictures and size distributions of titanium dioxide nanoparticles using in this research. The nanoparticles thus produced were calculated to have the average diameters of 30 nm.

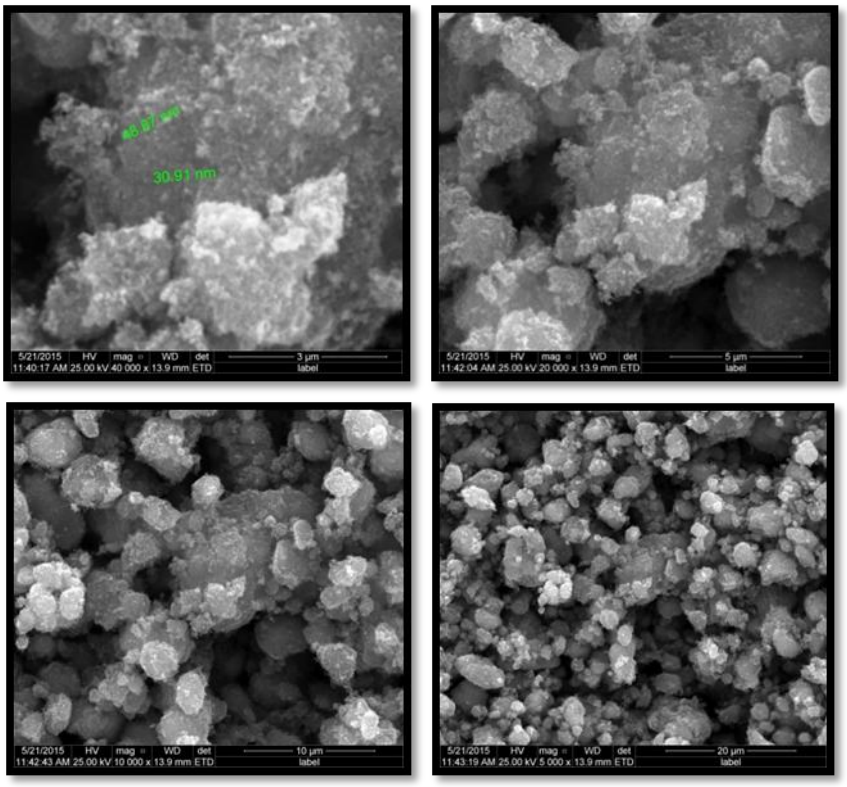

Figure 3. SEM pictures and size distributions of titanium dioxide nanoparticles

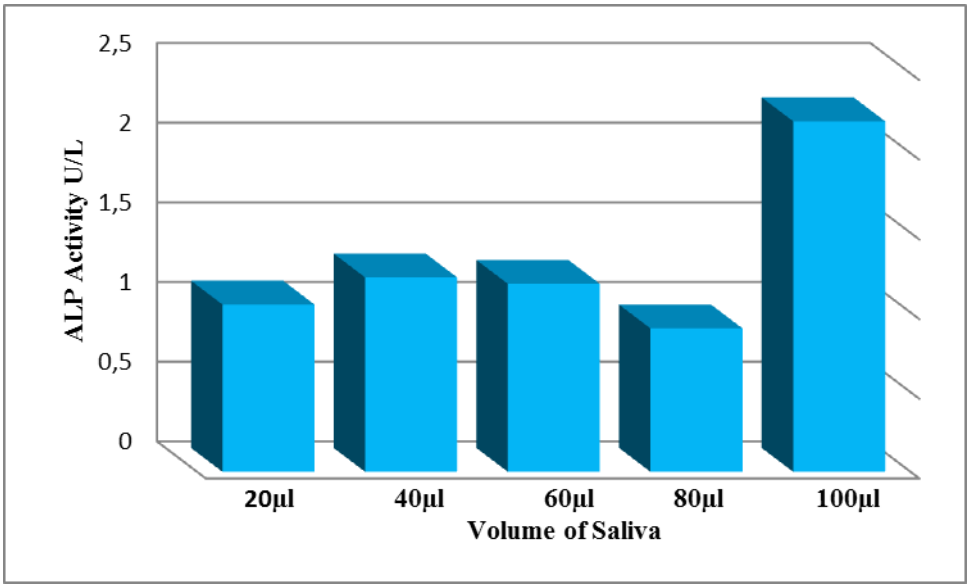

Figure 4. Effect of saliva volume on ALP activity

From the results in Figure 4, it is concluded that 100 µl of saliva is the best volume for measuring the ALP activity according to the conditions of experiments. The kinetic biochemical tests revealed that NPs of TiO2 caused the inhibition effect on the salivary ALP activity as shown in Figure 5. The observed results show that any increase in TiO2 NPs concentration caused decreasing in percentage of inhibition of enzyme activity. The greater inhibition of TiO2 NPs on enzyme activity was at concentration 0.15 µg/ml in total volume 1.370 ml of solvent as shown in Figure 6.

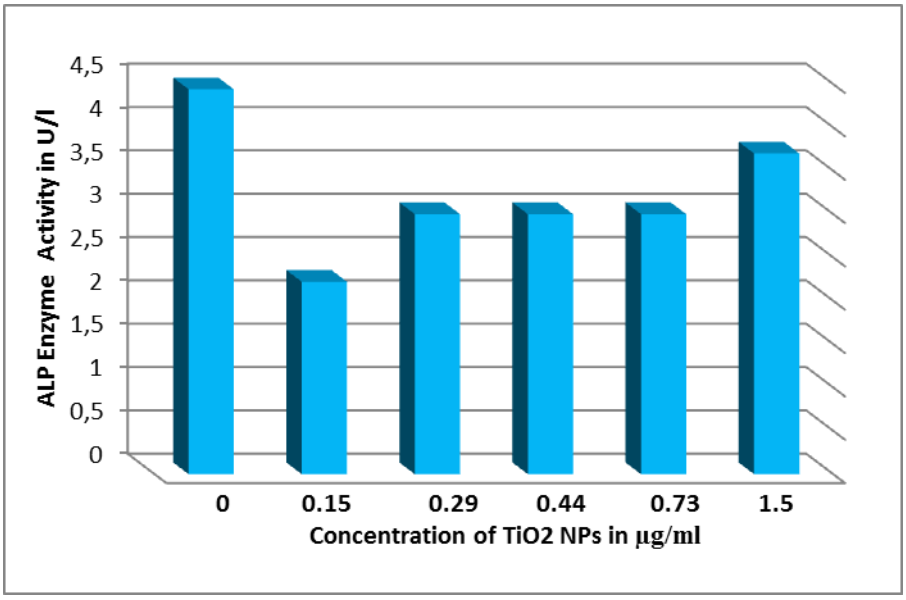

Figure 5. Salivary ALP activity in presence of different concentration of TiO2 NPs

The greater percentage of inhibition of TiO2 NPs on enzyme activity was 50 % at concentration 0.15 µg/ml as a final concentration as seen in Figure 6.

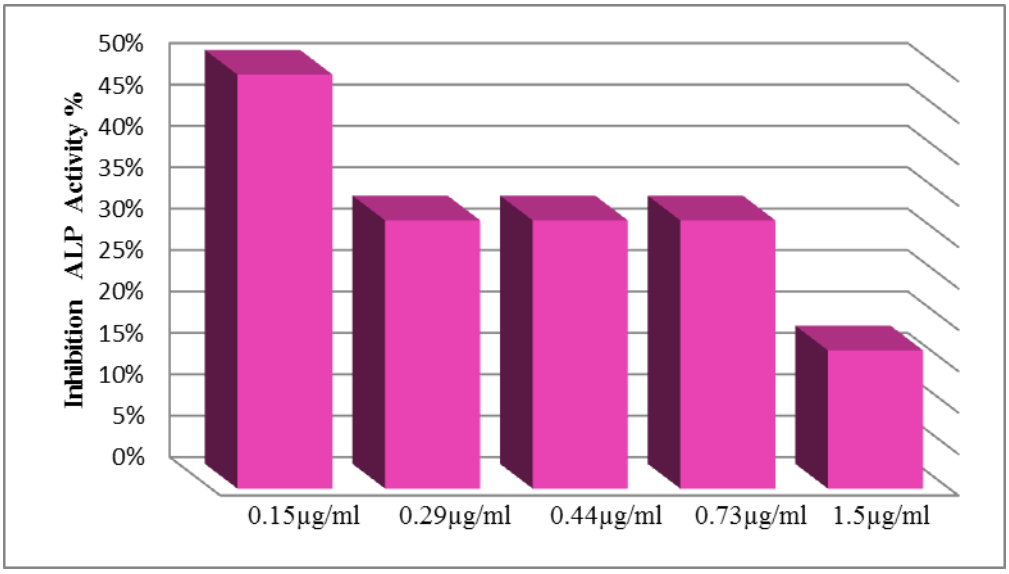

Figure 6. Percentage inhibition of salivary ALP activity in different concentrations of TiO2 NPs

In recent study of Al-Rubaee et al. [21] on the effect of Au and Ag nanoparticles on acid phosphatase activity, similar inhibition effect was obtained, the greater inhibition of Au NPs on ACP activity in sera of healthy subjects was 5 % at concentration 5.7 µg/ml and Ag nanoparticles was 5.8 % at concentration 10 µg/ml. Another study on the effect of silver nanoparticles on salivary LDH activity observed that any increase in Ag nanoparticles concentration caused increasing in percentage of inhibition of enzyme activity and the greater inhibition of Ag NPs on enzyme activity was 40.1 % at concentration 7.5 µg/ml [22].

Schug et al. results [23] show that in intact heterotrophic biofilms, the alkaline phosphatase activity was not affected following exposure to surface functionalized TiO2 NPs and UV radiation. While, an alkaline phosphatase enzyme isolated from E. coli was powerfully inhibited at lower concentrations of titanium dioxide nanoparticles than the intact biofilms.

We need many studies in order to investigate and explain the cause of high inhibition of TiO2 NPs on ALP activity in lower range of concentrations, and determine the type of inhibition.

To try to realize the possible effect of TiO2 NPs on salivary ALP activity in patients with gingivitis the activity measured with and without NPs and compared with that of control group. The results shown in Table 2.

Table 2: Mean and standard deviation for salivary ALP activity in Gingivitis patients with and without TiO2 NPs and control group

Groups	**Salivary ALP Activity in U/L Mean ± SD**
Control group	0.74±0.77
Gingivitis group without NPs	1.49±1.34
Gingivitis group with NPs	0.72±0.76

Table 3: Significance level among the three groups*

	df	P value
Control - Gingivitis	19	0.036
Gingivitis - TiO2NPs	19	0.000
Control - TiO2NPs	10	0.916

* Control group which represent measurement the salivary ALP activity in healthy subject without TiO2 NPs and gingivitis group, that represent ALP activity in patients with gingivitis without [TiO2 NPs] and the third group, salivary ALP activity in patients with gingivitis with [0.15 µg/ml] of TiO2 NPs as a final concentration

Statistical analysis comparing between the ALP activity of the three groups of this study revealed a significant difference [$P< 0.05$] between control and gingivitis as the ALP activity increase in gingivitis. This result agree with many results from other studies as in Yoshie et al. [24] that showed an increase in the alkaline phosphatase activity in the severe stage of periodontal diseases, and after treatment, the activity of this enzyme was restored to the normal value found in healthy persons. There are some suggestions to explain this increase. Yan et al. [25] show the increase in ALP enzyme activity may be due to their release by inflammatory cells and bacterial cells into gingival crevicular fluid and consequently into saliva. This result agree with Numabe et al. [26] who show that changes in enzymatic activity of salivary ALP activity reflect metabolic changes in the gingiva in inflammation [26]. While other observations [26, 27] suggest that a significant amount of alkaline phosphatase levels present in saliva is produced locally by diseased periodontal tissues. The ALP levels can be considered as potential indicator for periodontal disease [27, 28]. Mojgan and Afsanehin [29] show that there is unusual conditions, like loss of alveolar bone due to periodontitis, the activity of salivary ALP may demonstrate a significant rise, which is very important biomarker for periodontal problems.

The same statistical analysis comparing between the [gingivitis - TiO2 NPs] group, a highly significant difference $P<0.001$ as a result for inhibition of ALP activity by titanium dioxide nanoparticles. While for the third group [Control - TiO2 NPs] statistical analysis revealed a

nonsignificant difference P> 0.05 as the ALP activity increase in gingivitis and inhibited by TiO2 nanoparticles.

Conclusion

In conclusion, the salivary ALP activity was inhibited, a highly significant, by lower concentration of TiO2 NPs [0.15 µg\ml] more than the upper range of concentrations and this need another study to explain it. Enzyme levels in saliva of gingivitis patients were significantly high than the control.

References:

1. American Academy of Periodontology: Drug-associated gingival enlargement. Informational paper. J Periodontal (2004); 75:1424-1431

2. Lindhe J, Karrying T and Lang N: Clinical periodontology & implant dentistry, fifth edition, (2008) Vol. 2, Clinical concepts, Chapter 26: pp. 573-586.

3. Catalina P, Camelia S, and Monica B. Growth factors and Connective Tissue Homeostasis in Periodontal Disease, NurcanBuduneli (Ed), ISBN (2012); 978-953-307-924-0.

4. Mariotti A.: Dental plaque induced gingival disease. Ann. periodontal. (1999); 4(1):7-17.105.

5. Saini R, Marawar, PP; Shete S et al. Periodontitis a true infection. J Global Infect Dis. (20096); 2:149-50.

6. Rosalki SB, Mcintyre N. Biochemical investigation in the management of liver disease. Oxford textbook of clinical hepatology, 2nd edition. New York, Oxford University press (1999); p. 503-521.

7. Chapple I, Garner I, Saxby M, Moscrop H, Matthews J. Prediction and diagnosis of attachment loss by enhanced chemiluminescent assay of crevicular fluid ALP levels. Journal Clinical Periodontal. (1999); 26:190-8.

8. Gao J, Symons AL, Haase H and Bartold PM. Should cementoblasts express ALP activity? Preliminary study of rat cementoblasts in vitro. J Periodontal. (1999); 70(9):951-9.

9. Shibata Y, Yamashita Y, Miyazaki H, Ueno S, Takehara T. Effective method of discriminating between oral bacterial and human ALP activity. Oral Microbiol Immunol. (1994) Feb; 9: 35-9.

10. Yan F. ALP level in gingival crevical fluid of periodontitis before and after periodontal treatment. Chung Hua Kou Chiang Hseueh Tsa China. (1995); 30: 255-266.

11. Albrecht MA, Evans CW and Raston CL. Green chemistry and the health implications of nanoparticles. J Green Chem. (2006); 8: 417-420.

12. Kim JS, Kuk E, Yu KN, Kim JH, Park SJ, Lee HJ, et al. Antimicrobial effects of silver nanoparticles. NanomedNanotechnolBiol Med (2007); 3: 95-101.

13. Bhupendra C, Anjana K, Nidhi A and updhyay RV. Highly bacterial resistant silver nanoparticles: synthesis and antibacterial activities. J. Nano pat. Res., 10, Janury. (2010).

14. Chandra G, Ghosh KS, Dasgupta S and Roy A. Evidence of conformational changes in adsorbed lysozyme molecule on silver colloids. International J. of Biological Macromolecules. (2010); 47(3):361-365.

15. Allaker RP. The Use of Nanoparticles to Control Oral Biofilm Formation. J Dent Res (2010); 89: 1175-1186.

16. Giertsen E. Effects of mouth rinses with triclosan, zinc ions, copolymer, and sodium lauryl sulphate combined with fluoride on acid formation by dental plaque in vivo. Caries Res (2004); 38: 430-5

17. Winkler, Jochen. Titanium Dioxide. Hannover: Vincent Network. (2003); pp. 5. ISBN 3-87870-148-9.

18. Loe H, Silness J. Periodontal disease in pregnancy. I. Prevalence and severity. J Acta Odontol Scand 1963;21, 533-551.

19. Silness J, Loe H. Periodontal disease in pregnancy. II. Correlation between oral hygiene and periodontal condition. J Acta Odontol Scand 1964; 22, 121-135.

20. Chen L, Rahme K, Holmes JD, Morris MA and Slater KH. Non-solvolytic synthesis of aqueous soluble TiO2 nanoparticles and real-time dynamic measurements of the nanoparticle formation. Nanoscale Research Letters (2012); 7:297.

21. AL-Rubaee E, Ali A, Salman A, Salman Z. Inhibition Effect of Noble Metals Nanoparticles on Acid Phosphatase Activity in sera of healthy subject. Accepted to publish in Eng. and Technology J. (2014).

22. AL-Rubaee E. Kinetic study of the effect of gold and silver Nanoparticles on salivary LDH activity. GJSR Journal. (2014); Vol. 2(4), pp. 111-118.

23. Schug H, Isaacson CW, Sigg L, Ammann AA, Schirmer K. Effect of TiO2NPs and UV radiation on extracellular enzyme activity of intact heterotrophic biofilms. Environ Sci Technol. (2014); 48 (19):11620-8.

24. Yoshie H, Tai H, Kobayashi T, Oda-Gou E, Nomura Y, Numabe Y. Salivary enzyme levels after Scaling and Interleukin 1 genotypes in Japanese patients with chronic periodontitis. Journal Periodontal (2007); 78:498-503. Back to cited text no. 3

25. Yan F, Cao C, Li X. Alkaline phosphatase level in gingival crevical fluid of periodontitis before and after periodontal treatment. Zhonghua Kou Qiang Yi XueZaZhi (1995); 30:255-66. Back to cite text no. 11 (PUBMED).

26. Numabe Y, Hisano A, Kamoi K, Yoshie H, Ito K, Kurihara H. Analysis of saliva for periodontal diagnosis and monitoring. Periodontology (2004); 40: 115-9. 25.

27. Nakashima K. Roehrich N. Cimasini G. Osteocalcin. - Prostaglandin E2 and alkaline phosphatase in gingival crevicular fluid: their relations to periodontal status. J ClinPeriodontol. (1994); 21(5):327-33.

28. Kibayashi M, Tanaka M, Nishida N, Kuboniwa M, Kataoka K, Nagata H, et al. Longitudinal study of the association between smoking as a periodontitis risk and salivary biomarkers related to periodontitis. Journal Periodontol (2007); 78(5):859-67.

29. Mojgan P, Afsaneh R. Salivary biochemical markers of periodontitis. Rom J Biochem (2013); 50:129-46.

Published in the Russian Federation
European Journal of Molecular Biotechnology
Has been issued since 2013.
ISSN: 2310-6255
E-ISSN: 2409-1332
Vol. 10, Is. 4, pp. 197-209, 2015

DOI: 10.13187/ejmb.2015.10.197
www.ejournal8.com

UDC 537.523, 612(075)

S. Miller's Experiments in Modelling of Non-Equilibrium Conditions with Gas Electric Discharge Simulating Primary Atmosphere

[1] Ignat Ignatov
[2] Oleg Mosin

[1] The Scientific Research Center of Medical Biophysics (SRCMB), Bulgaria
Professor, D. Sc., director of SRCMB
1111, Sofia, N. Kopernik street, 32
E-mail: mbioph@dir.bg
[2] Moscow State University of Applied Biotechnology, Russian Federation
Senior research Fellow of Biotechnology Department, Ph. D. (Chemistry)
103316, Moscow, Talalihina ulitza, 33
E-mail: mosin-oleg@yandex.ru

Abstract

In this paper are submited data on the possibility of applying the coronal gas discharge effect (CGDE) in modeling non-equilibrium conditions with gas electric discharge simulating conditions occurying in the primary atmosphere (electric sparks, lightning) imitating S. Miller's experiments. The physical basis and technique of visualization of gas discharge (GD) glowing of water drops in alternating electric fields of high electrical voltage (5–30 kV) and frequency (10–150 kHz), as well as the possible electrosynthesis of organic molecules from a mixture of inorganic substances as hydrogen (H_2), methane (CH_4), ammonia (NH_3) and carbon monoxide (CO) in aqueous solutions of water exposed under the electrical discharge, UV-radiation and thermal heating to t = +100 °C were examined. The colour coronal spectral gas discharge analysis was applied for investigation of water samples of various origin, the samples of hot mineral, sea and mountain water obtained from various water sources of Bulgaria.

Keywords: coronal gas discharge effect, primary atmosphere, water, origin of life, S. Miller's experiments.

Introduction

Coronal gas discharge effect (CGDE) is observed by the characteristic glowing of corona electrical discharge (flooding, crown, streamer) on the surface of objects being placed in the alternating electric field of high frequency (10–150 kHz) and electric voltage (5–30 kV) [1]. In this process in the ionization zone develops the corona gas discharge sliding on the dielectric surface, occurring in a nonuniform electric field near the electrode having a small radius of curvature. With decreasing in the degree of heterogeneity of the electric field (the radius of curvature of the electrode ~1–3 mm) and with increasing of electric voltage the corona electrical discharge takes not uniform, but streamer (sometimes flare or spray) form. In this case, the electrically active processes are removed off at a distance of 10–20 cm from the surface of the electrode.

In the scientific literature, along with the terms of coronal gas discharge (CGD) are used gas discharge (GD), electric frequency (EFD) discharge, selective high frequency electric (SHFED) discharge etc. [2].

Coronal gas discharge glowing has found some scientific and practical applications in biophysics, as well as other branches of science [3] and technology [4]. Its advantages include safety, sterility, clarity and interpretability of the data obtained, ease of storage and subsequent computer processing, the ability to monitor the development of processes in time, comparing the structural, functional and temporal processes, etc.

Scientific and fundamental aspects of the coronal gas discharge effect and its scientific value consists in the fact that the CGD creates in laboratory conditions a selective electrical gas discharge, similar to the natural occuring electrical plasma phenomena (lightning) and electrostatic discharge on the surface of biological and organic objects, as well as inorganic samples of different nature including water drops [5]. Over the past decade, using the energy of the electric field in laboratory conditions from inorganic substances has been synthesized a variety of organic compounds – amino acids, proteins, nucleosides [6]. In those experiments (S. Miller's experiments, USA) were simulated the non-equlibrium processes with different sources of energy ocuring in primary anoxic atmosphere in which was possible the synthesis of organic molecules from inorganic ones due to the energy of spark electrical discharges (electrosynthesis), short-wave UV radiation from the Sun and other sources of geothermal energy [7].

The aim of this research was to explore the possibility of coronal gas discharge effect in modeling non-equilibrium conditions with gas electric discharge simulating electrical processes going on in primary atmosphere and forecasting the possible electrochemical reactions occurring in water by means of the treatment by the electric field of high intensity and frequency.

Material and Methods

Objects for Study

By using the method of coronal gas discharge spectral analysis were treated and analyzed hot mineral water samples containing bicarbonate (HCO_3^-) anions, cations of alkali metals (Na^+, K^+, Ca^{2+}, Mg^{2+}, Zn^{2+}) and water with varrying content of HDO, derived from various Bulgarian sources.

Non-Equilibrium Gas Discharge Experiments

Experiments were caried out by using selective high-frequency electric discharge (SHFED) on a device with the electrode made of polyethylene terephthalate (PET, hostafan) with an electric voltage on the electrode 15 kV, electric impulse duration 10 μs, and electric current frequency 15 kHz. The electrode of the device was made of hostafan, and was filled up with electro-conductive fluid. The spectral range of the emission was in the range λ = 380–495 nm and λ = 570–750±5 nm. The measurements were measured in electronvolts (eV). Detection of gas disharge glowing was conducted in a dark room equipped with a red filter. Along with the visible range, for this method were obtained color spectra in UV and IR range. Evaluation of the characteristic parameters of snapshots was based on the analysis of images treated by standard software package.

Statistical Processing of the Experimental Data

Evaluation of the characteristic parameters was carried out on the basis of the analysis of the images processed by a standard software package. Statistical processing of the experimental data was performed using the statistical package STATISTISA 6 using a Student's *t*-criterion (at $p < 0,05$).

Results and Discussion

Basic Aspects of Gas Electric Discharge Effect

For generation of gas electric discharge edffect are used special electric devices generating electromagnetic field of high frequency and voltage [8]. Schematic diagram of a typical device is shown in Figure 1. The device contains the generator of electric field and an electrode made from PET or hostaphan. At the electrode is applied alternating electrical field with frequency of 15 kHz and voltage 15 kV (in other methods, these values are assumed to be equal 0,2–15 kHz and 5–

30 kV). The studied object is grounded by a conductor, and placed on the electrode between which and the object is formed insulator, i.g. a thin layer of air which molecules undergo dissociation under the influence of the electromagnetic field generated by the electrode.

In this thin air layer with thickness of ~10–100 μm formed between the studied object and the electrode are developed the following processes [9]:

– Excitation, polarization and ionization by the electric field of high electric voltage and frequency the main components of air – the molecules of nitrogen (78 % N_2), oxygen (21 % O_2) and carbon dioxide (0,046 % CO_2). In the result of this is formed an ionized gas, i.e. gas with separated electrons having negative charges, creating a conductive medium, i.g. plasma;

– Formation of a weak electric current in the form of free moving electrons separated from molecules of N_2, O_2 and CO_2, which generate gas discharge between the studied object and the electrode. The form of gas discharge glowing, its density and surface brightness distribution is determined mainly by electromagnetic properties of the object;

– The transition of electrons from lower to higher energy levels and back again, during which there emanates a discrete quantum of light radiation in the form of photon emission. The transition energy of electrons depends on the external electric field and the electronic state of the material of the studied object. Therefore, in different areas surrounding the electric field, the electrons receive different energy impulses, i.e. "skipping" at different energy levels that result in emission of light photons with different wavelengths (frequencies) and the energy, coloring the contour of the glow in various spectral colors.

Processes outlined above form the gas discharge effect, allowing study the electrical properties of the object at its interaction with an external electromagnetic field [10]. It was demonstrated that electrical conductivity of the object – the reciprocal of electrical resistance, expressed in siemens, has virtually no effect on the formation of GD-glow which depends mostly on the dielectric constant.

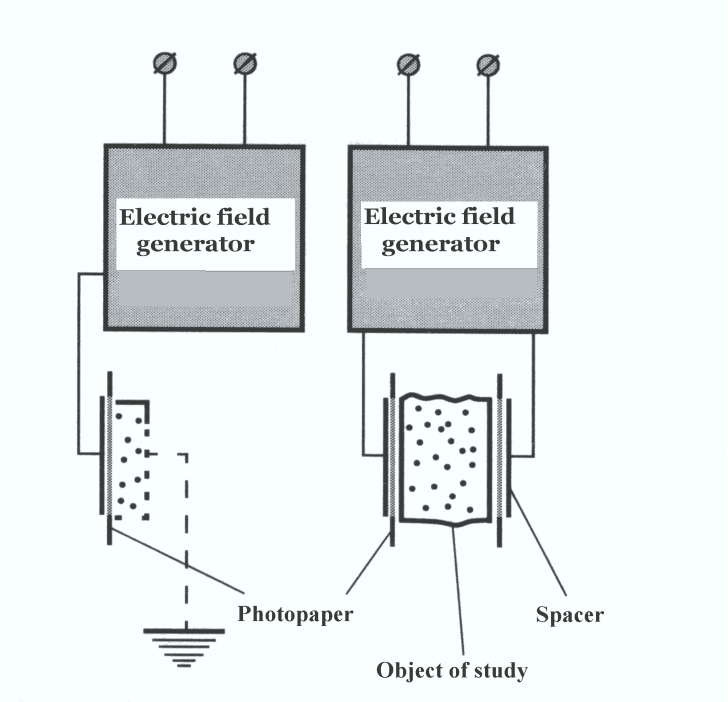

Figure 1: Schematic diagram of the electric device for visualizing of GD-glow

Dependence of the electrical conductivity σ ($Ohm^{-1} \cdot m^{-1}$) and the thermal conductivity K ($W/m \cdot K$) is determined by the Wiedemann-Franz law:

$$\frac{K}{\sigma} = \frac{\pi^2}{3}\left(\frac{k}{e}\right)^2 T, \quad (1)$$

where k – Boltzmann constant (1,380662 · 10^{-23} J/K); e – electron charge (-1,02176 · 10^{-19} Kl), T – temperature (K).

For the calculation of the basic physical parameters of the gas discharge is used the experimental dependence of the conductivity per unit area of the recording medium on the following parameters of the electric discharge:

$$\sigma = a - [U_p \frac{(d_2 + \delta)}{\delta \cdot d_2} \varepsilon_0 \frac{(d_2 + \delta)}{\delta \cdot d_2}], \quad (2)$$

where: $\delta = \frac{d_1}{\varepsilon_1} + \frac{d_3}{\varepsilon_3}$;

α – slope rate of electrical impulse;
T – duration of the electrical impulse;
U_p – breakdown voltage of the air layer gap between the sobject and the recording medium;
d_1 – width of the object;
d_2 – width of the zone of action of the electric field;
d_3 – width of the recording medium;
ε_0 – dielectric permittivity of the air (ε_0 = 1,00057 F/m);
ε_1 – dielectric permittivity of the studied object;
ε_3 – dielectric permittivity of the recording medium.

To calculate the breakdown voltage of the air layer is used this formula:

$$U_p = 312 + 6{,}2d_2 \quad (3)$$

As a result of mathematical transformations is obtained a quadratic equation describing the width of the air gap layer:

$$6{,}2d_2^2 + (\alpha T - 6{,}2\delta - 312)d_2 + 312\delta = 0, \quad (4)$$

This quadratic equation is reduced to the standard quadratic equation:

$$ax^2 + bx + c = 0, \quad (5)$$

where

$a = 6{,}2$; $b = \alpha T - 6{,}2\delta - 312$; $c = 312\delta$

This equation has two solutions:

$$x_{1,2} = \frac{-b \pm \sqrt{b^2 - 4ac}}{2a} \quad (6)$$

Correspondidly:

$$d_{1,2} = \frac{-[a \cdot T - 6{,}2\delta - 312] \pm \sqrt{[a \cdot T - 6{,}2\delta - 312)]^2 - 77{,}376\delta}}{12{,}4}, \quad (7)$$

The above equations allow calculate the maximum and the minimum width of the air gap layer for the occurrence of the elecric discharge with which help is being formed the electrical image of the studied object, which spectrum is shown in Figure 2 depending on the energy of the emitted light photons. Other gas discharge characteristics for various objects vary in character and light intensity, size of contour glow and color spectrum and depend both on its own electromagnetic radiation and the dielectric constant of the object. The intensity depends on the electric voltage applied on the electrode.

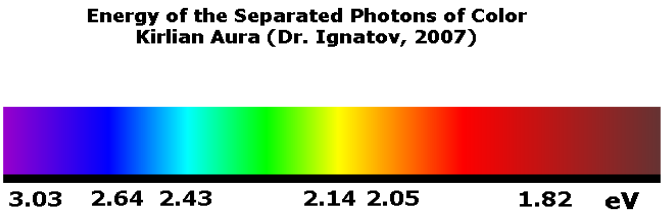

Figure 2: Spectrum of coronal gas discharge spectral analysis and the corresponding energy of the emitted photons (eV) (I. Ignatov, 2007)

As showed by the experiments [11], the characteristics of GD-glow of different biological objects vary in characteristics and intensity of light, size and color, and depend both on its own electromagnetic radiation and the dielectric constant of the object's material. GD-glowing intensity depends on the electric voltage of an electric current applied to the electrode. At low values of the electric voltage GD-emission does not occur, and at too high voltage there is a threat of dielectric breakdown, which is highly undesirable in experimental studies. Small electric current frequency can also cause dielectric breakdown. The optimum lower limit frequency of the electric current in this method is taken to be equal to 500 Hz, depending on the electrical potential difference between the electrode and the dielectric. Thus, for a standard glass electrode (glass as a dielectric material) is possible with low voltage electrical current to obtain the characteristic GD-glowing at the lower limit of the electric frequency at ~200 Hz. The upper frequency limit for the electric current lies between ~15 kHz and ~20 kHz, and mainly depends on the electrical parameters of the electrode material. Between the lower and upper bound are observed two characteristic intense peaks: at ~650 Hz and at ~7000 Hz. In the first case, at a low frequency of the electric current plays an important role permittivity. In the second case – at a high frequency of electric current, the electrical conductivity of the object is not important, but more important is the object's own electromagnetic field, which is not uniform, and is not in direct relation with the electrical conductivity. As an electrode may be used a plate made of a rigid polymeric material (epoxy, PET hostafan, polyester) coated on one side with a thin electrically conductive copper layer. In this case the function of a dielectric performs the polymer material. In order to avoid the dielectric breakdown at the edges of the dielectric, the layer of copper at ~10 mm from the edge of the electrode is removed. The electrode treated in this way is suitable for use with high voltage electrical current.

The process of photographing objects is carried out in a dark room or at a red light filter. On the dielectric plate, serving as an electrode creating the electric field of high voltage, is placed a sheet of light sensitive paper or a film. The object under study (water droplets) is placed on the top of the film. Between the studied object and the dielectric plate is applied the pulsating electric voltage from the electromagnetic field generator. At the electric field with high voltage and frequency in the air gap zone of the contact between the object and the plate there develops gas electrical discharge (avalanche or slide) characterized by GD-glow around the object – corona electrical discharge at the wavelength λ = 380–490 nm and λ = 560–780 nm, illuminates the photo paper or the film. After developing photographic paper most striking areas become darker which is typical for the photographic process. Since the investigated object is in contact with the photo paper (in the form of a circle in the center), this area is not illuminated.

In Bulgarian Scientific Research Center of Medical Biophysics to visualize the GD-glowing is developed the method of the selective high frequency electric discharge (SHFED) performed with using the electrode of a polymer material hostafan characterized by high dielectric strength (160–200 kV/mm). Photographing of GD-glow in this methodology is one of the physical methods, in which the image quality when using the film is higher than using the "Polaroid" camera or digital computer methods. The electrical voltage applied to the electrode of the device makes up ~15 kV at a frequency of electric current at ~15 kHz. This makes it easy to obtain and carry out the parametric analysis of GD-image. This method was used in the modeling non-equilibrium conditions with gas electric discharge simulating primary atmosphere.

Modeling of Non-Equilibrium Conditions with Gas Electric Discharge

The first experiments on the modeling of non-equilibrium conditions with gas electric discharge simulating primary atmosphere and electrosynthesis of organic substances by the energy of the electric field in a primary oxygen-free atmosphere were held in 1953 by S. Miller (USA) [12]. For this aim the mixture of water and gases consisted of hydrogen (H_2), methane (CH_4), ammonia (NH_3) and carbon monoxide (CO) was placed into a closed glass container being exposed by pulsating electrical spark discharges at the temperature of boiling water; oxygen was not allowed into the unit. After processing the reaction mixure by the electric discharge it was found that from the initial inorganic substance was synthesized organic compounds – aldehydes and amino acids. Experiments found that approximately ~10–15 % of carbon was transferred into an organic form. However, about ~2 % of carbon was detected in the amino acids, the most common of which was glycine. Initial analysis showed the presence in the reaction mixture obtained after the processing

by spark electric discharge 5 amino acids. A more complete analysis carried out in 2008 [13], showed the formation by electrosynthesis in the reaction mixture 22 amino acids having from 5 to 20 carbon atoms in the molecule (Figure 3). Interestingly is that along with the amino acids in the reaction mixture after the treatment with electric spark discharges were detected trace amounts of nucleo bases.

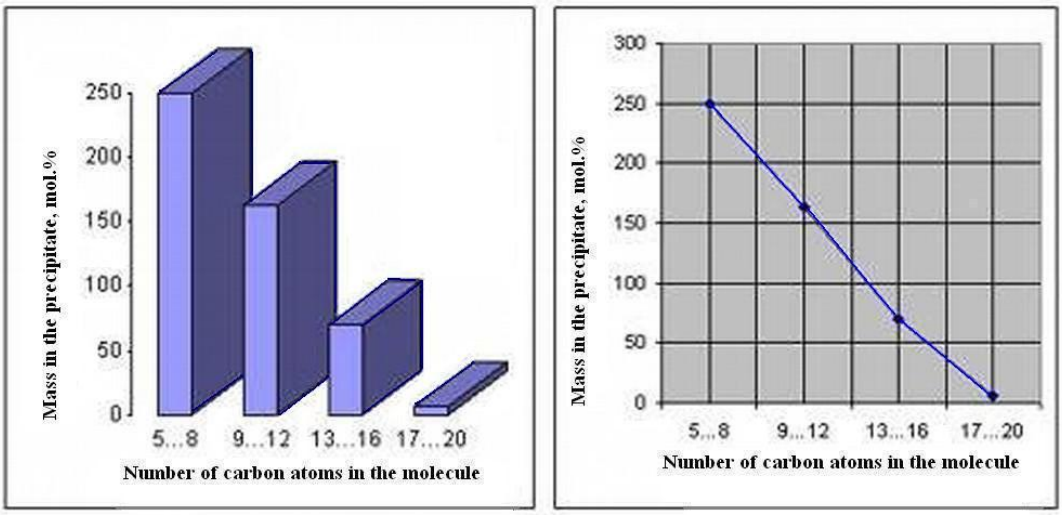

Figure 3: Distribution of carbon compounds obtained in the experiments of S. Miller, the mass and the number of carbon atoms in the molecule (diagrams constructed by the authors according to the S. Miller experiments)

S. Miller's experiments were reproduced in different variations with a combination of electrical discharges, UV-radiation and heat. Thus, in aquous solutions of formaldehyde (CH_2O) with hydroxylamine (NH_2OH), formaldehyde with hydrazine (N_2H_4) and HCN, after heating a reactionary mixture to +95 ^oC were detected amino acids [14]. In model experiments reaction products were polymerized into short peptide chains that is the important stage towards inorganic synthesis of protein. In a reactionary mixture of water with 4-aminoimidazole-5-carboxamidine, 4-aminoimidazole-5-carboxamide, NH_3, formamidine and urea at heating to +95 ^oC were synthesized purines (Figure 4). In 1960 A Wilson [15] after processing by the electric spark discharge of water vapor, ammonia (NH_3), hydrogen sulfide (H_2S), sulfur and yeast ash, obtained in the reaxion mixture the larger organic polymer molecules containing 20 or more carbon atoms. These polymers in aqueous solutions formed thin films with surface area of ~1 cm^2, resembling surfactants concentrated on the surface of the air-water interface (Figure 5). It is assumed that these films of polymer molecules were synthesized at the boundary between different phases, and played an important role in the early stages of the evolution of the first membrane-organized microstructures – the proteinoid microspheres [16] formed from thermal proteinoids at thermal treatment of the reaction mixture at temperatures of +95 ^oC. Thermal proteinoids are short protein-like molecules resembling early evolutionary forms of proteins. They are formed from amino acid mixtures subjected to influence of temperatures from +60 ^oC up to +170 ^oC, and consisted of 18 amino acids usually occurring in protein hydrolyzates. The synthesized proteinoids are similar to natural proteins on a number of other important properties, e.g. on linkage by nucleobases and ability to cause the reactions similar to those catalyzed by enzymes in living organisms as decarboxylation, amination, deamination, and oxidoreduction. Proteinoids are capable to catalytically decompose glucose [17] and to have an effect similar to the action of α-melanocyte-stimulating hormone [18]. The best results on polycondensation were achieved with the mixes of amino acids containing aspartic and glutamic acids, which are essential amino acids occurring in all modern living organisms. By morphological features the proteinoid microspheres with a diameter ~5–10 μm resemble cell membrane, which in certain conditions (pH = 4–5) may be double (Figure 6). The catalyst for their formation could serve sulfur and its derivatives which were found in ancient rocks in the form of grains of sulfides, as well as pyrite sands. Synthesis of protenoid microspheres from a mixture of thermal proteinoids is is important because it provides

material for the next stage of the evolution of life. This is the stage from disparate organic molecules to organized proteinoid molecules having the organized structure and separated from the surrounding environment by primitive membrane.

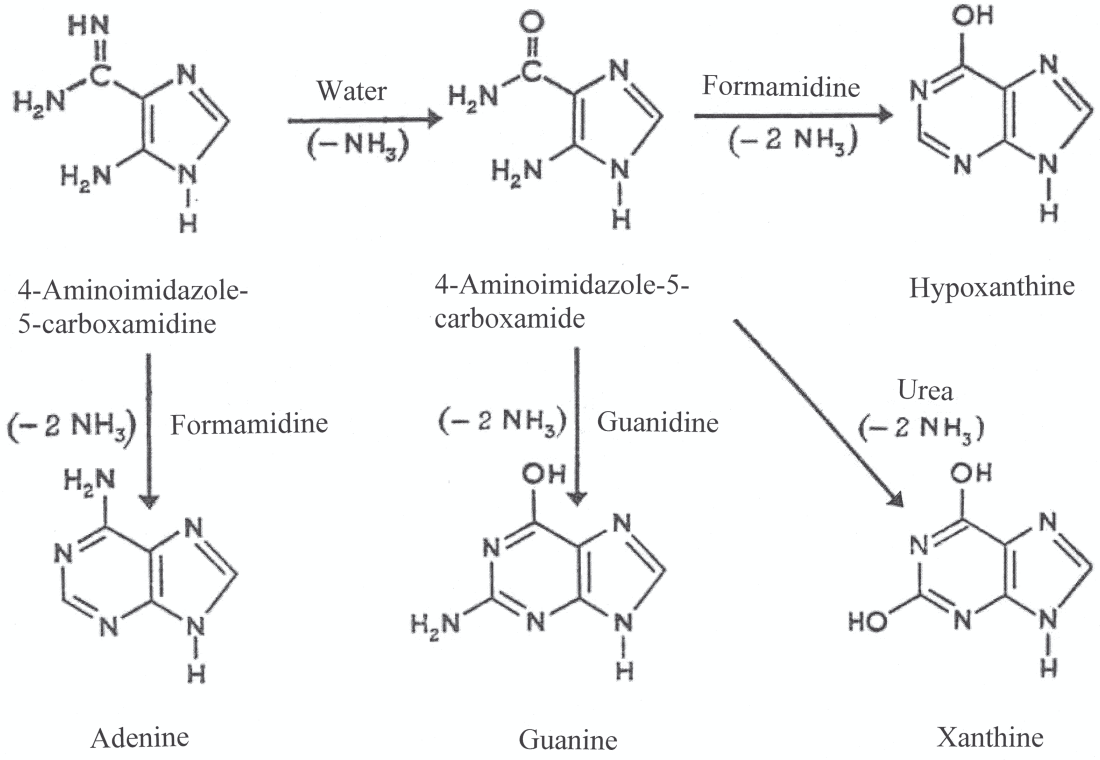

Figure 4: Prospective mechanisms of thermal (+95 °C) synthesis of purines – hypoxanthine, adenine, guanine and xanthine in aqueous solutions from their predesesors – 4-aminoimidazole-5-carboxamidine, 4-aminoimidazole-5-carboxamide, water, NH_3, formamidine and urea

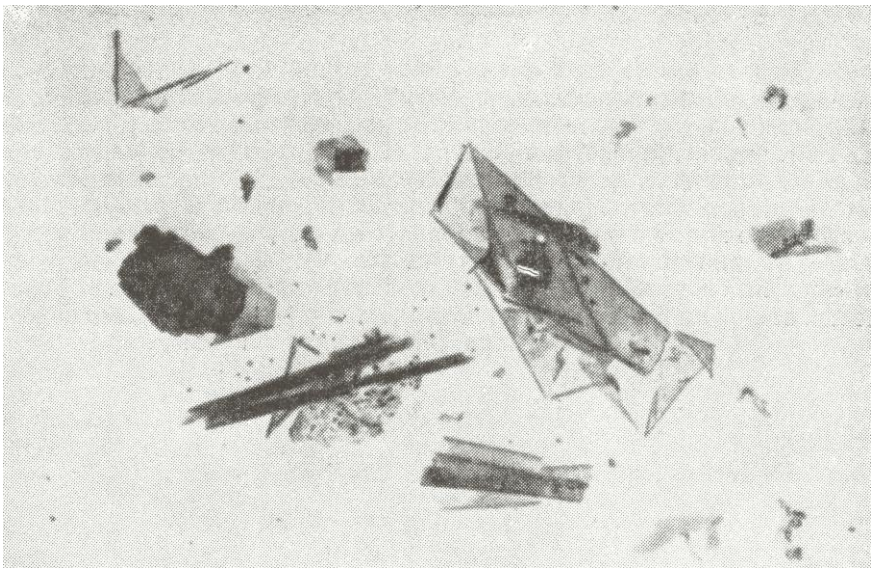

Figure 5: Thin films of organic polymers formed after the electrical spark discharges in a mixture of H_2O, NH_3, H_2S, sulfur and yeast ash [15]

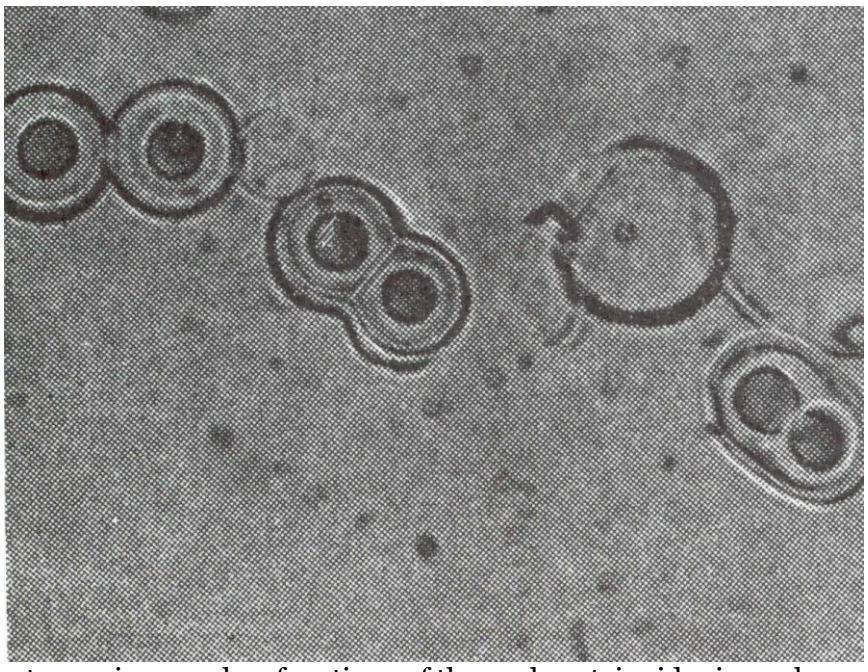

Figure 6: Electron micrographs of sections of thermal proteinoid microspheres in scanning electron microscope (magnification × ~1000 times) [16]

It should ne noted that in the implementation of the gas discharge effect as well as in experiments of S. Miller are modeled extreme non-equilibrium conditions with gas electric discharge, resulting that in a thin layer of air gap with thickness ~100 μm are formed reactive radicals reacting with each other to form new compounds (electrosynthesis). Such extreme conditions are thought to have occurred in the primary oxygen-free atmosphere of the Earth, which supposedly consisted of a mixture of water and gases – H_2, CH_4, NH_3 and CO, subjected to spark electrical discharges (lightning) under the conditions of high solar (UV) and geothermal activity.

According to our previous experiments, the first living structures may have evolved in warm and hot mineral water with a high content of bicarbonate (HCO_3^-) anions, cations of alkali metals (Na^+, K^+, Ca^{2+}, Mg^{2+}, Zn^{2+}) [19]. The similar composition and water temperature were modeled on the electrode of the gas discharge device made of hostafan, with electric voltage – 15 kV, electric impulse duration – 10 μs; electric current frequency – 15 kHz, wherein the air gap layer on the boundary with water sample was formed the electrical gas discharge, similar to plasma phenomena (lightning) and electrostatic discharge on the surface of organic and inorganic samples of various kinds. The investigated water sample before being placed onto the electrode was heated up to the boiling point temperature and then cooled. In preliminary experiments in the interelectrode space was formed a semblance of an organized structure with dimentions ~1,2–1,4 mm (Figure 7). In the control sample of water on the electrode the structure was not organized. With increasing the length of the gas electric discharge, the structure was somewhat increased in size. Moreover, in experiments was observed formation of small structures and their further "adjoining" to the larger structure This experiment shows that, under certain external conditions (gas electrical discharge, heat) it is possible the structural organization of water. It should be noted that water in natural conditions is heated up to +100 °C by the magma. The structure formed from the thermoheated water was evidently a result of self-organization. Living organisms are complex self-organizing systems. Thermodynamically they belong to the open systems because they are constantly exchanging substances and energy with the environment. The changes in the open systems are relatively stable in time. The stable correlation between components in thermodynamic open system is called a dissipative structure. According to I. Prigozhin, the formation of dissipative structures and the elaboration to living cells is related to changes in entropy [20]. Taking these results into consideration, it is possible to conclude that the initial stage of evolution, apparently, was connected with the formation at high temperature the mixures of amino acids and nitrogenous substances – analogues of nucleic acids. Such synthesis is possible in aqueous solutions under thermal conditions in the presence of H_3PO_4 as a catalyst. The next stage is polycondensation of

amino acids into thermal proteinoids at temperatures 65–95 °C. After that stage in a mix of thermal proteinoids in hot water solutions are formed the membrane like structures – proteinoid microspheres. In 2011 T. Sugawara (Japan) created membrane like proto cells from aqueous solution of organic molecules, DNA and synthetic enzymes under temperature close to water's boiling point +95 °C [21]. These experiments are excellent confirmation of the possibility that first organic forms of life originated in hot water.

Figure 7: The organized structure in water sample subjected to the temperature +100 °C in the electric field of high voltage and frequency (I. Ignatov, 2014). The material of the electrode – hostafan; electric voltage – 15 kV, electric impulse duration – 10 μs; electric current frequency – 15 kHz

Study the GD-glowing of W*ater Drops in Electric Field* of High Voltage *and Frequency*

The exposure high-frequency electric discharge to water appears in the form of characteristic GD-glowing around water drops. From the physical point of view, this process is characterized by a process of non-equillibrium transport of electric discharge in adjacent to the object of study thin air gap being ionized by the electric field. The authors believe that the emergence of GD-glow around water drops may be explained by taking into account the energy of the electric field and the change due to the influence of the electric field on the water structure, which in turn may be due to intermolecular rearrangements within associative elements of water. This fact may indicate that the structural elements of water may pocess "information" properties.

The authors consider that it seems unlikely that life originated in the "chaotic" non-informative water. Living organisms and water are complex, self-organizing systems having a characteristic structure. According to recent data, water is an associated liquid consisting of associated elements – clusters with general formula $(H_2O)_n$, where n = 3–50 [22]. These associates can be described as unstable groups (dimers, trimers, tetramers, pentamers, hexamers etc.) in which individual H_2O molecules are linked by van der Waals forces, dipole-dipole and other interactions with charge transfer, including hydrogen H...O bonding [23]. At room temperature, the degree of association of H_2O molecules may vary from 2 to 21 or even more.

The hydrogen bond results from interaction between electron-deficient H-atom of one H_2O molecule (hydrogen donor) and unshared electron pair of an electronegative O-atom (hydrogen acceptor) on the neighboring H_2O molecule; the structure of hydrogen bonding, therefore may be

defined as $O...H^{\delta+}–O^{\delta-}$. As the result, the electron of the H-atom due to its relatively weak bond with the proton easily shifts to the electronegative O-atom. The O-atom with increased electron density becomes partly negatively charged – δ^-, while the H-atom on the opposite side of the molecule becomes positively charged – δ^+ that leads to the polarization of $O^{\delta-}–H^{\delta+}$ covalent bond. In this process the proton becomes almost bared, and due to the electrostatic attraction forces are provided good conditions for convergence of O...O or O...H atoms, leading to the chemical exchange of a proton in the reaction $O–H...O \leftrightarrow O...H–O$. Although this interaction is essentially compensated by mutual repulsion of the molecules' nuclei and electrons, the effect of the electrostatic forces and donor-acceptor interactions for H_2O molecule compiles 5–10 kcal per 1 mole of substance. It is explained by negligible small atomic radius of hydrogen and shortage of inner electron shells, which enables the neighboring H_2O molecule to approach the hydrogen atom of another molecule at very close distance without experiencing any strong electrostatic repulsion. In respect of energy hydrogen bond has an intermediate position between covalent bonds and intermolecular van der Waals forces, based on dipole-dipole interactions, holding the neutral molecules together in gasses or liquefied or solidified gasses. Hydrogen bonding produces interatomic distances shorter than the sum of van der Waals radii, and usually involves a limited number of interaction partners. These characteristics become more substantial when acceptors bind H-atoms from more electronegative donors. Hydrogen bonds hold H_2O molecules on 15 % closer than if water were a simple liquid with van der Waals interactions. The hydrogen bond energy compiles 5–10 kcal/mole, while the energy of O–H covalent bonds in H_2O molecule – 109 kcal/mole [24]. The values of the average energy ($\Delta E_{H...O}$) of hydrogen H...O-bonds between H_2O molecules make up 0,1067±0,0011 eV [25]. With fluctuations of water temperature the average energy of hydrogen H...O-bonds in water associates changes. Therefore, the hydrogen bonds in the liquid state are relatively weak and unstable: they can easily occur and collapse as a result of thermal fluctuations [26]. This process leads to structural inhomogeneity of water characterizing it as an associated heterogeneous two-phase liquid with short-range ordering, i.e. with regularity in mutual positioning of atoms and molecules, which reoccurs only at distances comparable to distances between initial atoms, i.e. the first H_2O layer. Changing the position of one structural element (H_2O molecules) under the influence of any external factor, or changing the orientation of the neighboring H_2O molecules ensures high sensitivity of the structural elements of water to various external influences (electromagnetic, thermal, sound fields, etc.).

H_2O molecules in the liquid state at standard conditions (1 atm, 22 ^oC) are able to perform oscillating movements about its axis of rotation, as well as random and directed movement, whereby individual molecules can be moved from one location to another through the volume of water via cooperative interactions. As a result, in aqueous solutions is possible autoprotoliz i.e. take off a proton H^+ from one molecule of water, followed by moving and adding H^+ to a neighboring molecule H_2O, leading to delocalization of a proton within a cluster to form a hydronium ion as H_3O^+, $H_5O_2^+$, $H_7O_3^+$, $H_9O_4^+$, etc. Hydrogen bonding leads to the formation of the next hydrogen bond and redistribution of electrons, which in its turn promotes the formation of the following hydrogen bond, which length increasing with distance. Cooperative hydrogen bonding increases the O–H bond length, at the same time causing a reduction in the H...O and O...O distances [27]. The protons held by individual H_2O molecules may switch partners in an ordered manner within hydrogen networks [28]. This property explains the extremely labile, mobile character of interaction of woter associates with each other. In the mathematical model of water it is assumed that water consists of a variety of association elements - neutral clusters $(H_2O)_n$ and charged cluster ions $[(H+)(H_2O)_n]^+$ and $[(OH-)(H_2O)_n]^-$ with different types of similarity which can form quasicrystalline structure, wherein *n* in mathematical calculations can reach tens or even hundreds of units [29]. This property explains the extremely labile, mobile character of the electrostatic interaction of associative elements of water with each other, due to which occures the construction of structural elements of water into hollow cells (clathrates) up to 0,5–1,0 μm.

Due to the fact that H_2O molecules are polar dipoles, they are thought to have oriented in the electric field. In the study of GD-glowing of water droplets it was proposed that electric glow was partly due to the polarity of H_2O molecules and their orientation by an external electric field [30]. Polarization is a physical phenomenon associated with electromagnetic waves, when the electromagnetic field oscillates (fluctuates) in one particular plane perpendicular to the direction of wave propagation. Water has the highest dielectric constant and it determines its chemical

properties as an universal solvent. GD-images of water drops of various origin and degree of purification indicate that the different water samples interact in different ways with the electric field. Moreover water is a source of super-weak and weak alternating electromagnetic radiation. In this case, it is possible the induction of the corresponding electromagnetic field and resonance effects of combination (superposition) of electromagnetic fields capable to altering the structural and functional characteristics of biological objects by 70–80 % consisting of water. As it was demonstrated by I. Ignatov (Figure 8), the character of GD-glowing of water drops placed in an alternating electric field of high voltage and frequency influences the origin of water sample, the method of the water treatment, the presence of impurities in water and other factors.

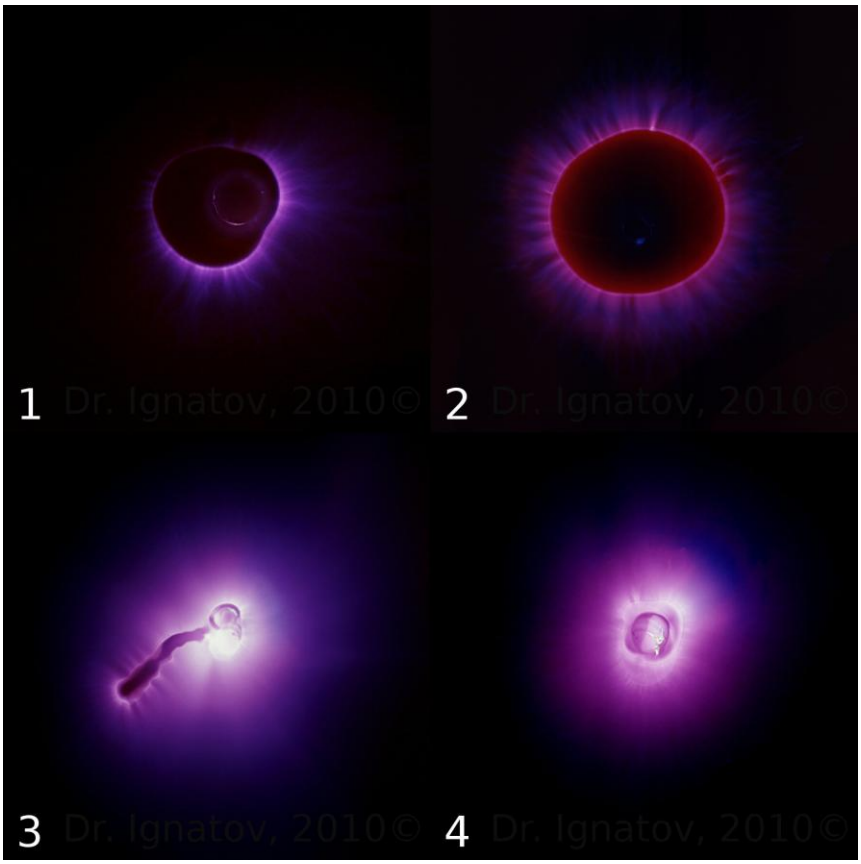

Figure 8: Color gas disharge spectral analysis of water droplets of different origin (I. Ignatov, 2012) (the electrode voltage – 15 kV, electric current frequency – 15 kHz): 1 – tap water; 2 – mountain water (Teteven, Bulgaria); 3 – seawater (Hammamet, Tunisia); 4 – Karst and mineral water (Zlatna Panega, Bulgaria)

The differences in the GD-glowing of different water samples can be caused by different structure and composition of water (cation-anion composition), physical and chemical properties (pH, conductivity, surface tension), which affects the differences in the interaction of water samples with the electric field. This method is not widely used in scientific research.

Conclusion

The data obtained suggest about the possibility of application of the selective gas discharge in modeling non-equilibrium conditions with gas electric discharge simulating electrical spark discharge processes going on in primary atmosphere, simulating S. Miller's experiments. In this process, within a thin layer of air border with 100 μm there occures the formation of reactive radicals interacting with each other to form new compounds (electrosynthesis). Such extreme conditions supposedly might take place in the primary anoxic Earth hydrosphere, consisting of a mixture of water and gases – H_2, CH_4, NH_3 и CO, subjected to the action of high-energy electrical discharges (lightning). The experiments showed that the most favorable for the emergence of first

organic forms and maintenance of biochemical reactions is hot mineral water interacting with $CaCO_3$.

References:

1. Kirlian S.D. Kirlian S.D. Method for receiving photographic pictures of different types of objects. USSR Patent № 106401.

2. Antonov A., Yuskeselieva L. Research of water drops with high-frequency electric discharge (Kirlian) effect // *Bulgarian Academy of Science. 1968. V.* 21(5). P. 34–36.

3. Gudakova G.Z. Study of parameters of gas discharge glow microbiological cultures // Journal for Applied Spectroscopy. 1988. V. 49. № 3. P. 56–59.

4. Lapitskiy V.N., Pesotskaya L.A. Estimation of influence of schungite room on the state of human health by the method of Kirlian // Scientific Paper. 2012. № 11. P. 1–7.

5. Skarja M., Berden M., Jerman I. The influence of ionic composition of water on the corona discharge around water drops // Journal of Applied Physics. 1988. V. 84. № 5. P. 2436–2442.

6. Ignatov I., Mosin O.V. Origin of life and living matter in hot mineral water // *Naukovedenie. 2013. V.* 2(6). P. 1–19 [in Russian] [Online] Available: URL: http://naukovedenie.ru/PDF/04tvn213.pdf (February 13, 2013).

7. Lazcano A., Bada J.L. The 1953 Stanley L. Miller experiment: fifty years of prebiotic organic chemistry // Origin of Life and Evolution of Biospheres. 2004. V. 33 (3). P. 235–242.

8. Pehek J.O., Kyler H.J., Faust D.L. Image modulatic corona discharge photography // Science. 1976. V. 194. № 4262. P. 263–270.

9. Ignatov I., Mosin O.V. Kirlian effect in study the properties of biological objects and water // *Biomedical electronics. 2012. №* 12. P. 13–21.

10. Marinov M., Ignatov I. Color Kirlian spectral analysis. Color observation with visual analyzer. Hanover: Euromedica. 2008. P. 57–59.

11. Ignatov I., Mosin O.V. Method for colour coronal (Kirlian) spectral analysis // *Biomedical Radio Electronics*. 2013. № 1. P. 38–47.

12. Miller S.L. A production of amino acids under possible primitive earth conditions // Science. 1953. V. 117. № 3046. P. 528–5299.

13. Johnson A.P., Cleaves H.J., Dworkin J.P., Glavin D.P., Lazcano A., Bada J.L. The Miller volcanic spark discharge experiment // *Science. 2008. V.* 322(5900). P. 404–412.

14. Harada I., Fox S.W. Thermal synthesis of natural amino acids from a postulated primitive terrestrial atmosphere // *Nature. 1964. V.* 201. P. 335–336.

15. Wilson A.T. Synthesis of macromolecules // Nature. 1960. V. 188. P. 1007–1009.

16. Nakashima T. Metabolism of proteinoid microspheres / Ed. T. Nakashima. In: Origins of life and evolution of biospheres. New York: Acad. Press, 1986. V. 20(3–4). P. 269–277.

17. Fox S.W., Krampitz G. Catalytic decomposition of glucose in aqueous solution by thermal proteinoids // *Nature. 1964. V.* 203. P. 1362–1364.

18. Fox S.W., Wang C.T. Melanocytestimulating hormone: Activity in thermal polymers of alpha-amino acids // *Science. 1968. V.* 160. P. 547–548.

19. Ignatov I., Mosin O.V. Modeling of possible processes for origin of life and living matter in hot mineral and seawater with deuterium // *Journal of Environment and Earth Science. 2013.* V. 3(14). P. 103–118.

20. Nikolis P., Prigozhin I. Self-organization in non-equilibrium systems. - Moscow: Mir, 1979, 512 p.

21. Sugawara T. Self-reproduction of supramolecular giant vesicles combined with the amplification of encapsulated DNA // *Nature Chemistry. 2011. V.* 1127. P. 775–780.

22. Ignatov I., Mosin O.V. Structural mathematical models describing water clusters // *Mathematical theory and modeling. 2013. V.* 3(11). P. 72–87.

23. Ignatov I., Mosin O.V. Isotopic composition of water and its temperature in the evolutionary origin of life and living matter // *Naukovedenie. 2013. V.* 1(14). P. 1–16 [in Russian] [Online] Available: URL: http://naukovedenie.ru/PDF/42tvn113.pdf (February 13, 2013).

24. Arunan E., Desiraju G.R., Klein R.A. Definition of the hydrogen bond // *Pure Appl. Chem.* 2011. V. 83(8). P. 1637–1641.

25. Antonov A., Galabova T. / in Reports from the 6th Nat. Conference of Biomedical Physics and Engineering. Sofia, 1992.

26. Ignatov I., Mosin O.V. Structural models of water describing the cyclic clusters // Micro- and Nanosystem Technique. 2014. № 3. P. 47–56.

27. Goryainov S.V. A model of phase transitions in double-well Morse potential: Application to hydrogen bond // *Physica B. 2012. V.* 407. P. 4233–4237.

28. Bartha F., Kapuy O., Kozmutza C., Van Alsenoy C. Analysis of weakly bound structures: hydrogen bond and the electron density in a water dimmer // *J. Mol. Struct. (Theochem). 2003. V.* 666. P. 117–122.

29. Ignatov I., Mosin O.V. Mathematical models describing the nanostructure of water and nanoclusters // *Nanoingenering, Izdatel'stvo Mashinostroenie, Moscow*. 2013. №. 8. P. 32–46.

30. Ignatov I., Mosin O.V. Color coronal (Kirlian) spectral analysis in modeling of nonequilibrioum conditions with the gas electric discharges simulating primary atmosphere. S. Miller's experiments // *Naukovedenie. 2013. V.* 3(16). P. 1–15 [in Russian] [Online] Available: URL: http://naukovedenie.ru/PDF/05tvn313.pdf (May 10, 2013).

УДК 537.523, 612(075)

Эксперименты С. Миллера по моделированию неравновесных условий с коронным газовым электрическим разрядом, имитирующим первичную атмосферу

[1] Игнат Игнатов
[2] Олег Викторович Мосин

[1] Научно-исследовательский центр медицинской биофизики (НИЦМБ), Болгария
Профессор, доктор наук Европейской академии естественных наук (Германия)
директор НИЦМБ
1111, София, ул. Н. Коперника, 32/6
E-mail: mbioph@dir.bk
[2] Московский государственный университет прикладной биотехнологии, Российская Федерация
Старший научный сотрудник кафедры биотехнологии, канд. хим. наук.
103316, Москва, ул. Талалихина, 33
E-mail: mosin-oleg@yandex.ru

Аннотация. В статье представлены данные о возможности применения эффекта газоразрядного свечения (ГР) в моделировании неравновесных условиях с газовым электрическим разрядом, имитирующих условия, происходящие в первичной атмосфере Земли (электрические искры, молнии), иммитирующие эксперименты С. Миллера. Рассмотрены физические основы и методика визуализации ГР-свечения капли воды в переменном электрическом поле высокой электрического напряжения (5–30 кВ) и частоты (10–150 кГц), а также возможные реакции электросинтеза органических молекул из смеси неорганических веществ в водных растворах, как водород (H_2), метан (CH_4), аммиак (NH_3) и окись углерода (CO), подвергающихся воздействию электрического разряда, УФ-излучению и тепловому нагреву до t = +100 ^{0}C. Цветной корональной спектральный анализ был применен для исследования проб воды различного происхождения, а также образцов горячей минеральной, морской и горной воды, полученной из различных источников Болгарии.

Ключевые слова: электрический газовый разряд, первичная атмосфера, вода, происхождение жизни, эксперименты С. Миллера.

Published in the Russian Federation
European Journal of Molecular Biotechnology
Has been issued since 2013.
ISSN: 2310-6255
E-ISSN: 2409-1332
Vol. 10, Is. 4, pp. 210-227, 2015

DOI: 10.13187/ejmb.2015.10.210
www.ejournal8.com

UDC 735.29: 573.552

Studying the Hydrological Conditions for Origin of First Organic Forms of Life in hot Mineral Water with HDO

[1] Ignat Ignatov
[2] Oleg Mosin

[1] The Scientific Research Center of Medical Biophysics (SRCMB), Bulgaria
Professor, D. Sc., director of SRCMB
1111, Sofia, N. Kopernik street, 32
E-mail: mbioph@dir.bg
[2] Moscow State University of Applied Biotechnology, Russian Federation
Senior research Fellow of Biotechnology Department, Ph. D. (Chemistry)
103316, Moscow, Talalihina ulitza, 33
E-mail: mosin-oleg@yandex.ru

Abstract

The isotopic composition, the temperature and the pH value of water were analyzed in experiments with prognosis of primary hydrosphere and hydrological conditions for origin of first organic forms in hot mineral water with HDO. For this aim we performed experiments with hot mineral water and seawater from Bulgaria and water with varying content of deuterium using IR- and DNES-spectroscopy. As model systems were used cactus juice of *Echinopsis pachanoi* and Mediterranean jellyfish *Cotylorhiza tuberculata*. The reactions of condensation–dehydration occurring in alkaline aqueous solutions at t = 65–95 °C and pH = 9–10, resulting in synthesis from unorganic molecules the larger organic molecules as polymers and short polipeptides, were discussed, as well as the possible mechanisms of the deuterium accumulation in form of HDO in hot water. It was shown that hot alkaline mineral water with temperature from +65 °C to +95 °C and the pH value from 9 to 11 is more suitable for the origination of life and living matter than other analyzed water samples. In hot mineral waters the local maximums in IR-spectra are more manifested compared to the local maximums obtained in IR-spectra of the same water at a lower temperature. The difference in the local maximums from +20 °C to +95 °C at each +5 °C according to the Student *t*-criterion makes up $p < 0,05$.

Keywords: deuterium, hydrosphere, evolution, origin of life, IR spectroscopy, DNES.

Introduction

Previous biological experiments with D_2O and structural-conformational studies with deuterated macromolecules, performed by us, enable to modeling conditions under which the first living forms of life might be evolved [1–3]. The content of deuterium in hot mineral water may be increased due to the physical chemical processes of the deuterium accumulation. It can be presumed that primary water might contain more deuterium at early stages of evolution of first

living structures, and deuterium was distributed non-uniformly in the hydrosphere and atmosphere [4]. The primary reductive atmosphere of the Earth consisted basically of gas mixture CO, H_2, N_2, NH_3, CH_4, lacked O_2–O_3 layer protecting the Earth surface from rigid short-wave solar radiation carrying huge energy capable to cause radiolysis and photolysis of water. The processes accompanying accumulation of deuterium in the hydrosphere are solar radiation, volcanic geothermal processes and electric discharges in the atmosphere. These natural processes could lead to the enrichment of the hydrosphere by deuterium in the form of HDO which evaporates more slowly then H_2O, and condenses faster. If this is true, this is a significant fact regarding thermal stability of deuterated macromolecules in the preservation of life under thermal conditions, because chemical bonds with participation of deuterium are stronger than those ones formed of hydrogen.

The natural prevalence of deuterium makes up approximately 0,015–0,020 atom%, and depends strongly on the uniformity of substance and the total amount of matter formed in the course of early Galaxy evolution [5]. The average ratio of $D/^1H$ in nature makes up approximately 1:5700. In natural waters, the deuterium is distributed irregularly: from 0,02–0,03 mol.% for river water and sea water, to 0,015 mol.% for water of Antarctic ice – the most purified from deuterium natural water containing in 1,5 times less deuterium than that of seawater. According to the international SMOW standard isotopic shifts for D and ^{18}O in sea water: $D/^1H = (155{,}76\pm0{,}05)\cdot10^{-6}$ (155,76 ppm) and $^{18}O/^{16}O = (2005{,}20\pm0{,}45)\cdot10^{-6}$ (2005 ppm). For SLAP standard isotopic shifts for D and ^{18}O in seawater make up $D/^1H = 89\cdot10^{-6}$ (89 ppm) and for a pair of $^{18}O/^{16}O = 1894\cdot10^{-6}$ (1894 ppm). In surface waters, the ratio $D/^1H = \sim(1{,}32–1{,}51)\cdot10^{-4}$, while in the coastal seawater – $\sim(1{,}55–1{,}56)\cdot10^{-4}$. The natural waters of CIS countries are characterized by negative deviations from SMOW standard to $(1{,}0–1{,}5)\cdot10^{-5}$, in some places up to $(6{,}0–6{,}7)\cdot10^{-5}$, but however there are also observed positive deviations at $2{,}0\cdot10^{-5}$.

The constant sources of deuterium are explosions of nova stars and thermonuclear processes frequently occurring inside the stars. Probably, it could explain a known fact, why the amount of deuterium is slightly increased during the global changes of climate in warming conditions. The gravitational field of the Earth is insufficiently strong for the retaining of lighter hydrogen, and our planet is gradually losing hydrogen as a result of its dissociation into interplanetary space. Hydrogen evaporates faster than heavy deuterium, which can be collected by the hydrosphere. Therefore, as a result of this natural process of fractionation of H/D isotopes throughout the process of Earth evolution there should be an accumulation of deuterium in the hydrosphere and surface waters, while in the atmosphere and in water vapour deuterium content tends to be low. Thus, on the planet there occurs a natural process of separation of H and D isotopes, playing an essential role in the maintenance of life on the planet.

The second point regards the influence of temperature on the biochemical processes in living matter. Our recent studies have shown that the most favorable for the origin of life and living matter seem to be hot alkaline mineral waters interacting with $CaCO_3$ [6, 7]. According to the law for conservation of energy the process of self-organization of primary organic forms in water solutions may be supported by thermal energy of magma, volcanic activity and solar radiation. According to J. Szostak, the accumulation of organic compounds in small isolated lakes is more possible compared to the ocean [8]. It is most likely that life originated near a hydrothermal vent: an underwater spout of hot water. Geothermal activity gives more opportunities for the origination of life. In 2009 A. Mulkidjanian and M. Galperin demonstrate that the cell cytoplasm contains potassium, zinc, manganese and phosphate ions, which are not particularly widespread in the sea aquatorium [9]. J. Trevors and G. Pollack proposed in 2005 that the first cells on the Earth assembled in a hydrogel environment [10]. Gel environments are capable of retaining water, oily hydrocarbons, solutes, and gas bubbles, and are capable of carrying out many functions, even in the absence of a membrane. Hydrocarbons are an organic compounds consisting entirely of hydrogen and carbon. The data presented in this paper show that the origination of living matter most probably occurred in hot mineral water. This may occurred in ponds and hydrothermal vents in seawater or hot mineral water. An indisputable proof of this is the presence of stromatolites fossils. They lived in warm and hot water in zones of volcanic activity, which could be heated by magma and seem to be more stable than other first sea organisms [11].

Therefore, the purpose of the research was studying the hydrological conditions of primary hydrosphere (temperature, pH, isotopic composition) for possible processes for origin of first

organic forms in hot mineral water with HDO. Various samples of water from Bulgaria, as well water with varying deuterium content were studied within the frames of the research.

Material and methods

Chemicals

For preparation of water with varying content of deuterium (HDO) was used D_2O (99,9 atom.%) from the Russian Research Centre "Isotope" (St. Petersburg, Russian Federation). D_2O was preliminary distilled over $KMnO_4$ with the subsequent control of isotope enrichment by ^{1}H-NMR-spectroscopy on a Brucker WM-250 device ("Brucker", Germany) (working frequency: 70 MHz, internal standard: Me_4Si).

Biological Objects

The objects of the study were used the cactus juice of *Echinopsis pachanoi* and the Mediterranean jellyfish *Cotylorhiza tuberculata* (Chalkida, Greece, Aegean Sea).

Water Samples

The samples of water were taken from various water springs of Bulgaria:
1 – Mineral water (Rupite, Bulgaria);
2 – Seawater (Varna resort, Bulgaria);
3 – Mountain water (Teteven, Bulgaria);
5 – Deionized water (the control).
6 – Water with varrying deuterium content (HDO).

IR-Spectroscopy

IR-spectra of water samples were registered on Brucker Vertex ("Brucker", Germany) Fourier-IR spectrometer (spectral range: average IR – 370–7800 cm^{-1}; visible – 2500–8000 cm^{-1}; permission – 0.5 cm^{-1}; accuracy of wave number – 0.1 cm^{-1} on 2000 cm^{-1}) and on Thermo Nicolet Avatar 360 Fourier-transform IR (M. Chakarova).

DNES-Spectral Analysis

The research was made with the method of differential non-equilibrium spectrum (DNES). The device measures the angle of evaporation of water drops from 72 ° to 0 °. As the main estimation criterion was used the average energy ($\Delta E_{H...O}$) of hydrogen O...H-bonds between H_2O molecules in water's samples. The spectra of water were measured in the range of energy of hydrogen bonds 0,08–0,1387 eV with using a specially designed computer program.

High-Frequency Coronal Electric Discharge Experiments

A device for high-frequency coronal electric discharge was used in this study, constructed by I. Ignatov and Ch. Stoyanov. The frequency of the applied saw-tooth electric voltage was 15 kHz, and the electric voltage – 15 кV. The electric discharge was obtained using a transparent firm polymer electrode on which a liquid sample of water (2–3 mm) was placed. The spectral range of the photons released upon electric discharge was from λ = 400 to λ = 490 nm and from λ = 560 to λ = 700 nm.

Results and discussion

Studying Various Water Samples on the Feasibility for Origin of Life

We have carried out the research of various samples of mineral water obtained from mineral springs and seawater from Bulgaria (Fig. 1, curves *1–5*). For this aim we employed the IR-spectrometry and DNES method relative to the control – deionized water.

For calculation of the function *f(E)* represented the energy spectrum of water, the experimental dependence between the wetting angle (θ) and the energy of hydrogen bonds (E) is established:

$$f(E) = \frac{14{,}33\, f(\theta)}{[1-(1+bE)^2]^2}, \qquad (1)$$

where b = 14,33 eV^{-1}

The relation between the wetting angle (θ) and the energy (E) of the hydrogen bonds between H_2O molecules is calculated by the formula:

$$\theta = arcos\,(-1 - 14{,}33E) \qquad (2)$$

Cactus juice was also investigated by the DNES method (Fig. 1, *curve 1*). The cactus was selected as a model system because this plant contains approximately 90 % of water. The closest to the spectrum of cactus juice was the spectrum of mineral water contacting with Ca^{2+} and HCO_3^- ions (Fig. 1, *curve 2*). DNES-spectra of cactus juice and mineral water have magnitudes of local maximums (E, eV) at –0,1112; -0,1187; -0,1262; -0,1287 and –0,1387 eV. The similar local maximums in the DNES-spectrum between the cactus juice and seawater were detected at -0,1362 eV. The DNES-spectrum of the control sample of deionized water (Fig. 1, *curve 5*) was substantially different from DNES-spectra of seawater and mineral water.

Another important parameter was measured by the DNES method – the average energy ($\Delta E_{H...O}$) of hydrogen H...O-bonds among individual molecules H_2O, which makes up -0,1067±0,0011 eV. When the water temperature is changed, the average energy of hydrogen H...O-bonds alternates. This testified about the restructuring of average energies of hydrogen H...O-bonds among individual H_2O molecules with a statistically reliable increase of local maximums in DNES-spectra.

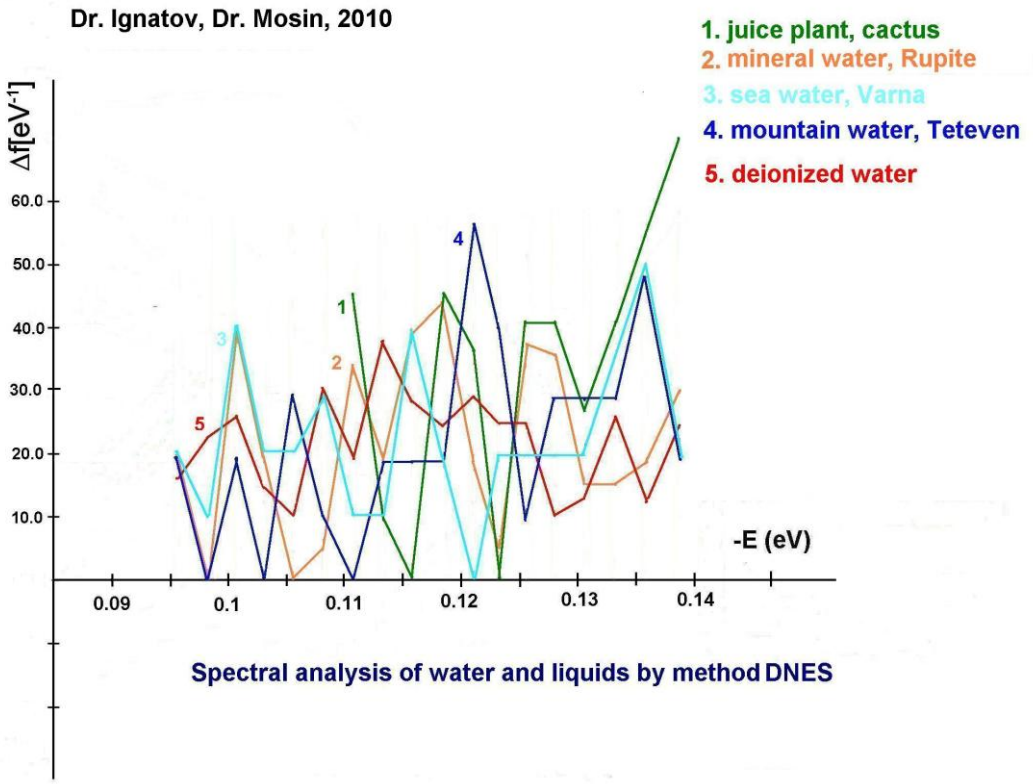

Figure 1: DNES-spectra of water samples of various origin: 1 – the cactus juice; 2 – mineral water from Rupite village (Bulgaria); 3 – seawater (Varna, Bulgaria); 4 – mountain water (Teteven, Bulgaria); 5 – deionized water (the control)

As it was shown from these experimental data, the closest to the IR-spectrum of the cactus juice was mineral water from Rupite Village (Bulgaria), which DNES and IR spectrum is shown in Fig. 2 and Fig. 3 (Thermo Nicolet Avatar 360 Fourier-transform IR). IR-spectra of cactus juice and mineral water containing HCO_3^- (1320–1488 mg/l), Ca^{2+} (29–36 mg/l), pH (6,85–7,19), have local

maximums at λ = 8,95; 9,67; 9,81; 10,47 and 11,12 μm (Fourier-IR spectrometer Brucker Vertex). Common local maximums in the IR-spectrum between the cactus juice and seawater are detected at λ = 9,10 μm. The local maximums obtained with the IR method at λ = 9,81 μm (*k* = 1019 cm^{-1}) and λ = 8,95 μm (*k* = 1117 cm^{-1}) (Thermo Nicolet Avatar 360 Fourier-transform IR) are located on the spectral curve of the local maximum at λ = 9,7 μm (*k* = 1031 cm^{-1}) (Fig. 3). With the DNES method were obtained the following results – (wave length λ, μm) 8,95; 9,10; 9,64; 9,83; 10,45 and 11,15 μm, or (wave numbers, *k*, cm^{-1}) 897; 957; 1017; 1037; 1099 and 1117 cm^{-1}.

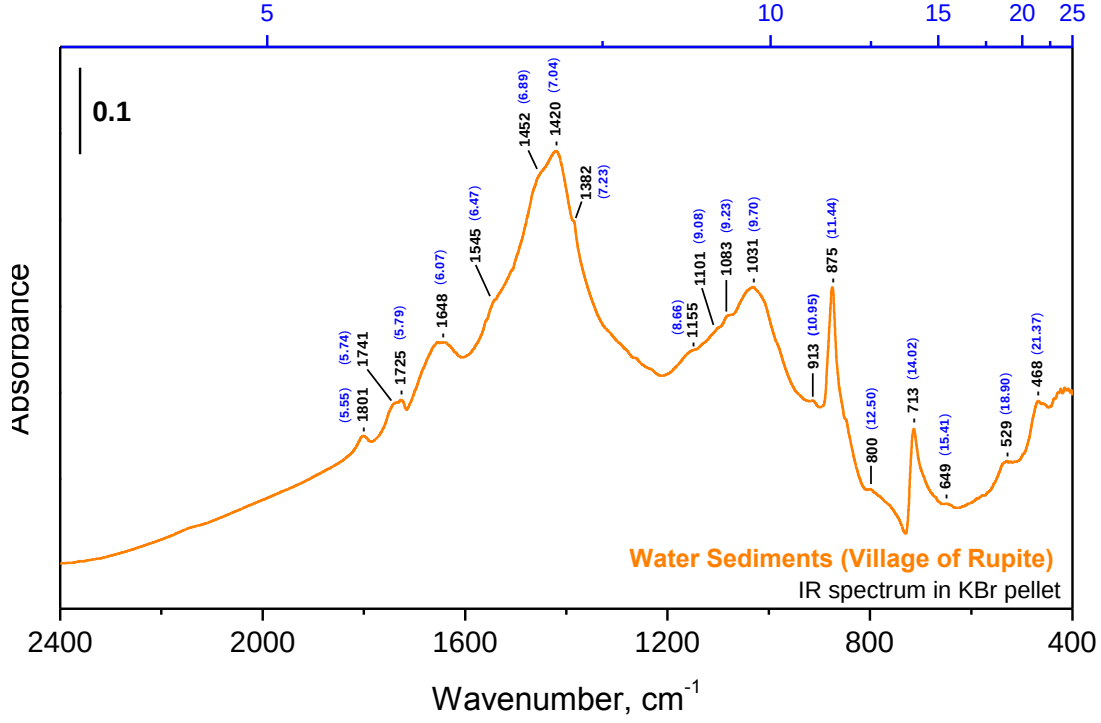

Figure 2: IR-spectrum of water sediments obtained from Rupite Village (Bulgaria)

Table 1: Characteristics of spectra of water of various origin obtained by DNES-method*

-E, eV			λ, μm	*k*, cm^{-1}
Cactus juice	**Mineral water from Rupite Village (Bulgaria)**	**Seawater**		
0,1112	0,1112	–	11,15	897
0,1187	0,1187	–	10,45	957
0,1262	0,1262	–	9,83	1017
0,1287	0,1287	–	9,64	1037
0,1362	–	0,1362	9,10	1099
0,1387	0,1387	–	8,95	1117

Notes:
*The function of the distribution of energies Δf was measured in reciprocal electron volts (eV^{-1}). It is shown at which values of the spectrum -E (eV) were observed the biggest local maximums of this function; λ – wave length; *k* – wave number.

The results with the Mediterranean jellyfish *Cotylorhiza tuberculata* indicated that the jellyfish has local maximums in IR-spectra at λ = 8,98 and λ = 10,18 μm (Fig. 3). Before measurements the jellyfish was kept in seawater for several days. On comparison the seawater has

a local maximum at λ = 8,93 μm in IR-spectra. These results were obtained with Thermo Nicolet Avatar 360 Fourier-transform IR. With DNES method the local maximums in spectra for jellyfish are detected at λ = 8,95 and 10,21 μm, and for seawater – at λ = 9,10 μm. A differential spectrum was recorded between jellyfish and seawater by using the Thermo Nicolet Avatar 360 Fourier-transform IR method. In the IR-spectrum of jellyfish are observed more pronouncedly expressed local maximums, detected by Thermo Nicolet Avatar 360 Fourier-transform IR and DNES method. The measurements demonstrate that two common local maximums are observed in IR-spectra of jellyfish and seawater. These maximums are not observed in the IR-spectrum of cactus juice and mineral water from Rupite (Bulgaria). Jellyfish contains approximately 97 (w/w) % of water and is more unstable living organism compared to those ones formed stromatolites. The explanation for this is the smaller concentration of salts and, therefore, the smaller number of local maximums in the IR-spectrum in relation to seawater.

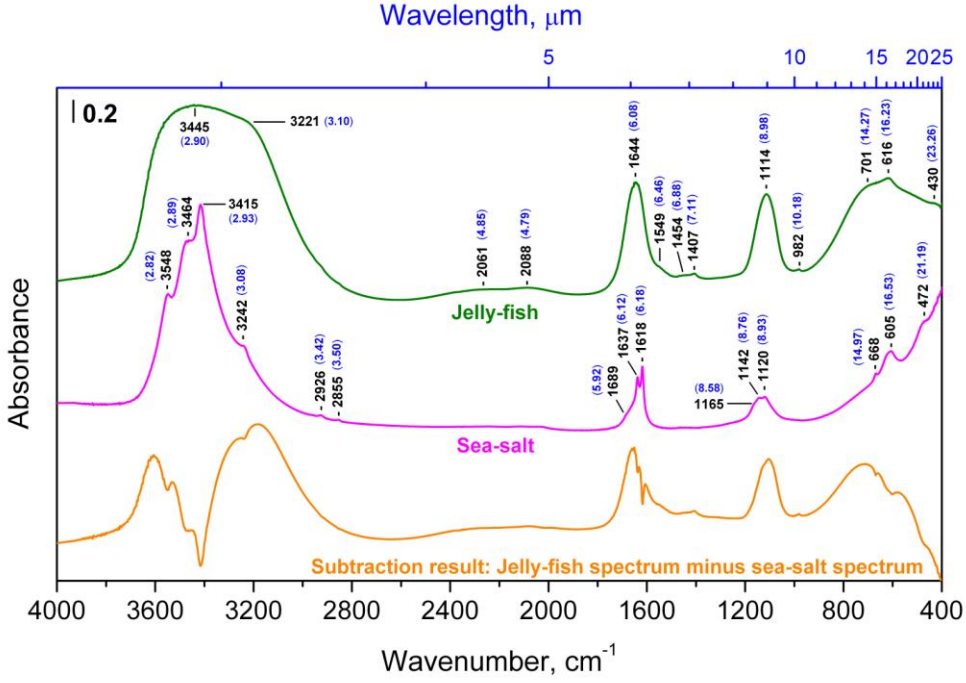

Figure 3: IR-spectrum of seawater obtained from Varna (Bulgaria) and jellyfish *Cotylorhiza tuberculata*, Chalkida (Greece), Aegean Sea

Such a character of IR- and DNES-spectra and distribution of local maximums may prove that hot mineral alkaline water is preferable for origin and maintenance of life compared to other types of water analyzed by these methods. Thus, in hot mineral waters the local maximums in the IR-spectrum are more manifested compared to the local maximums obtained in IR-spectrum of the same water at a lower temperature. The difference in the local maximums from t = +20 °C to t = +95 °C at each 5 °C according to the Student *t*-criterion makes up $p < 0,05$. These data indicate that the origination of life and living matter depends on the structure and physical chemical properties of water, as well as its temperature and pH value. The most closed to the IR- and DNES-spectrum of water, which contains bicarbonates and calcium ions typical for the formation of stromatolites is the IR-spectrum of cactus juice. For this reason cactus juice was applied as a model system. The most closed to local maximums in IR-spectrum of cactus juice are local maximums in IR-spectra of alkaline mineral water interacting with $CaCO_3$ and then seawater. In connection with these data the following reactions participating with $CaCO_3$ in aqueous solutions are important:

$$CO_2 + 4H_2S + O_2 = CH_2O + 4S + 3H_2O, \quad (3)$$

$$CaCO_3 + H_2O + CO_2 = Ca(HCO_3)_2, \quad (4)$$

$$CO_2 + OH^- = HCO_3^- \quad (5)$$

$$2HCO_3^- + Ca^{2+} = CaCO_3 + CO_2 + H_2O \quad (6)$$

The equation (3) shows how some chemosynthetic bacteria use energy from the oxidation of H_2S and CO_2 to S and formaldehyde (CH_2O). The equation (4) is related to one of the most common

processes in nature: in the presence of H_2O and CO_2, $CaCO_3$ transforms into $Ca(HCO_3)_2$. In the presence of hydroxyl OH^- ions, CO_2 transforms into HCO_3^- (equation (5)). Equation (6) is valid for the process of formation of the stromatolites – the dolomite layered acretionary structures formed in shallow seawater by colonies of cyanobacteria. In 2010 D. Ward described fossilized stromatolites in the Glacier National Park (USA) [13]. Stromatolites aged 3,5 billion years had lived in warm and hot water in zones of volcanic activity, which could be heated by magma. This suggests that the first living forms evidently evolved in hot geysers [14]. It is known that water in geysers is rich in carbonates, while the temperature is ranged from +100 ^oC to +150 ^oC. In 2011 a team of Japanese scientists under the leadership of T. Sugawara showed that life originated in warm or, more likely, in hot water [15]. From aqueous solution of organic molecules, DNA and synthetic enzymes were created proto cells. Under experimental conditions the initial solution was heated to a temperature close to the water's boiling point +95 ^oC. Then the temperature was lowered to +65 ^oC with formation of proto cells with primitive membrane. These experiments are excellent confirmation of the possibility that first organic forms of life originated in hot water.

The above-mentioned data can predict a possible transition from synthesis of small organic molecules under the temperatures +70–100 ^oC to more complex organic molecules as proteins. There are reactions of condensation-dehydration of amino acids into separate blocks of peptides that occur under alkaline conditions, with pH = 9–11. The important factor in reaction of condensation of two amino acid molecules into dipeptide is allocation of H_2O molecule when a peptide chain is formed. Because the reaction of polycondensation of amino acids is accompanied by dehydration, the H_2O removal from the reaction mixture speeds up the reaction rates. This testifies that formation of early organic forms may have occured nearby active volcanoes, because at early periods of geological history volcanic activity occurred more actively than during subsequent geological times. However, dehydratation accompanies not only amino acid polymerization, but also association of other small blocks into larger organic molecules, and also polymerization of nucleotides into nucleic acids. Such association is connected with the reaction of condensation, at which from one block a proton is removed, and from another – a hydroxyl group with the formation of H_2O molecule.

In 1969 the possibility of existence of condensation-dehydration reactions under conditions of primary hydrosphere was proven by M. Calvin [16]. From most chemical substances hydrocyanic acid (HCN) and its derivatives – cyanoamid (CH_2N_2) and dicyanoamid ($HN(CN)_2$) possess dehydration ability and the ability to catalyze the process of linkage of H_2O from primary hydrosphere [17]. The presence of HCN in primary hydrosphere was proven by S. Miller's early experiments [18]. Chemical reactions with HCN and its derivatives are complex with a chemical point of view; in the presence of HCN, CH_2N_2 and $HN(CN)_2$ the condensation of separate blocks of amino acids accompanied by dehydration, can proceed at normal temperatures in strongly diluted H_2O-solutions. These reactions show the results of synthesis from separate smaller molecules to larger organic molecules of polymers, e.g. proteins, polycarboxydrates, lipids, and ribonucleic acids (Fig. 4). Furthermore, polycondensation reactions catalyzed by HCN and its derivatives depend on acidity of water solutions in which they proceed [19]. In acid aqueous solutions with pH = 4–6 these reactions do not occur, whereas alkaline conditions with pH = 9–10 promote their course. There has not been unequivocal opinion, whether primary water was alkaline, but it is probable that such pH value possessed mineral waters adjoining with basalts, i.e. these reactions could occur at the contact of water with basalt rocks, that testifies our hypothesis.

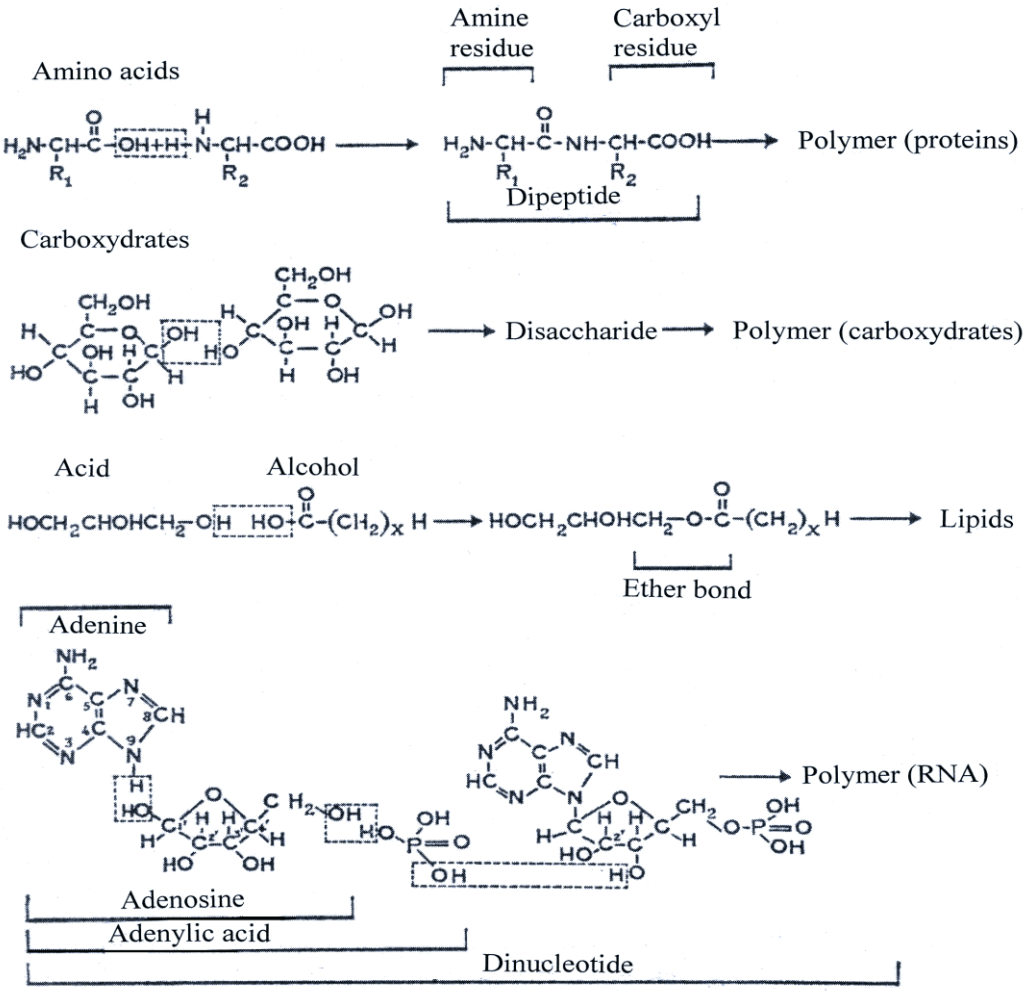

Figure 4: Possible reactions of condensation and dehydration in alkaline conditions with pH = 9–10 catalyzed by HCN and its derivatives, resulting in synthesis from separate molecules larger organic molecules of polymers. The top three equations: condensation and the subsequent polymerization of amino acids in proteins; carbohydrates – in polycarboxydrates and acids and ethers – into lipids. The bottom equation – condensation of adenine with ribose and H_3PO_4, leading to formation of dinucleotide

It should be noted, that geothermal sources might be used for synthesis of various organic molecules. Thus, amino acids were detected in solutions of formaldehyde CH_2O with hydroxylamine NH_2OH, formaldehyde with hydrazine (N_2H_4) in water solutions with HCN, after heating of a reactionary mixture to +95 °C [20]. In model experiments the reaction products were polymerized into peptide chains that are the important stage towards inorganic synthesis of protein. In a reactionary mixture with a HCN–NH_3 solution in water were formed purines and pyrimidines (Fig. 5). In other experiments amino acid mixtures were subjected to influence of temperatures from +60 °C up to +170 °C with formation of short protein-like molecules resembling early evolutionary forms of proteins subsequently designated as thermal proteinoids. They consisted of 18 amino acids usually occurring in protein hydrolyzates. The synthesized proteinoids are similar to natural proteins on a number of other important properties, e. g. on linkage by nucleobases and ability to cause the reactions similar to those catalyzed by enzymes in living organisms as decarboxylation, amination, deamination, and oxidoreduction. Proteinoids are capable to catalytically decompose glucose [21] and to have an effect similar to the action of α-melanocyte-stimulating hormone [22]. The best results on polycondensation were achieved with the mixes of amino acids containing aspartic and glutamic acids, which are essential amino acids occurring in all modern living organisms.

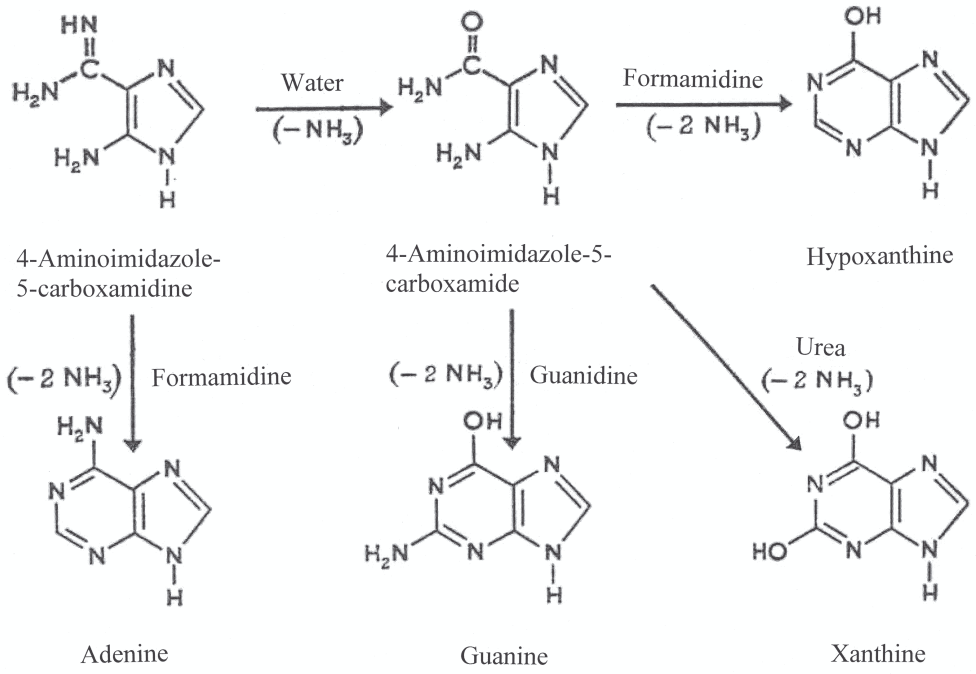

a)

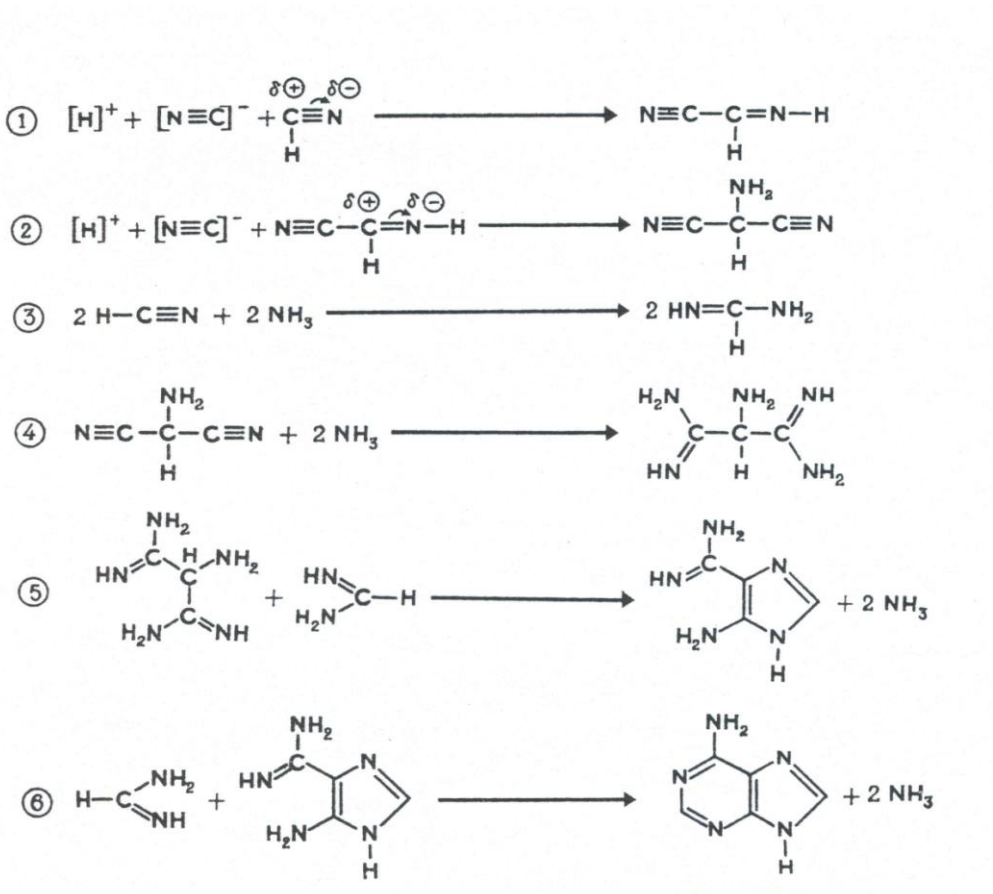

b)

Figure 5: Prospective mechanisms of thermal (+95 °C) synthesis of purines in aqueous solutions: *a)* – synthesis of hypoxanthine, adenine, guanine and xanthine from 4-aminoimidazole-5-carboxamidine, 4-aminoimidazole-5-carboxamide, water, NH_3, formamidine and urea; *b)* – synthesis of adenine from NH_3 and HCN (total reaction: 5HCN = adenine)

Under certain conditions (temperature, pH) in hot mixture of thermal proteinoids in water solutions are formed elementary structures like proteinoid microspheres with diameter 5–10 μm [23]. The best results on polycondensation were achieved with the mixes of amino acids containing aspartic and glutamic acids, which are essential amino acids occurring in all modern living organisms. By morphological features the proteinoid microspheres with a diameter ~5–10 μm resemble cell membrane, which in certain conditions (pH = 4–5) may be double (Fig. 6). The catalyst for their formation could serve sulfur and its derivatives which were found in ancient rocks in the form of grains of sulfides, as well as pyrite sands. Synthesis of protenoid microspheres from a mixture of thermal proteinoids is important because it provides material for the next stage of the evolution of life. This is the stage from disparate organic molecules to organized proteinoid molecules having organized structure and separated from the surrounding environment by the primitive membrane.

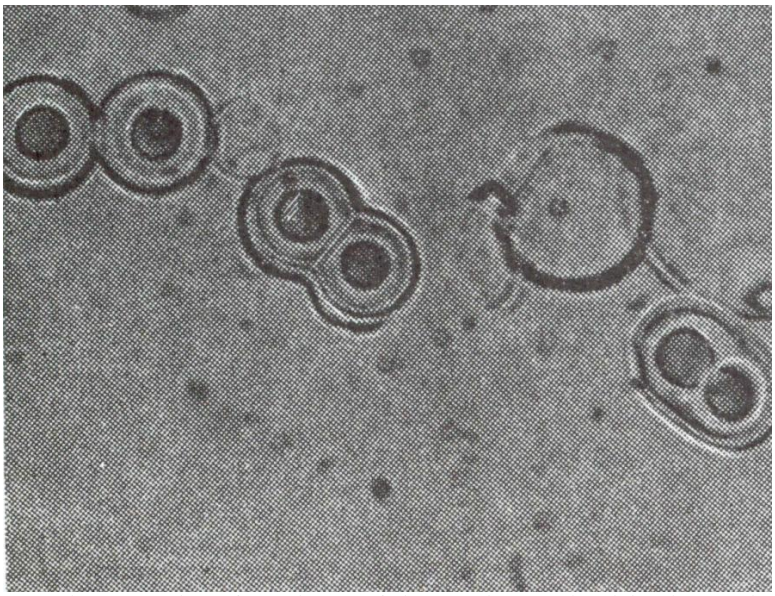

Figure 6: Electron micrographs of sections of thermal proteinoid microspheres in scanning electron microscope (magnification × ~1000 times) (Nakashima, 1987).

In further experiments was applied gas electric discharge analogous to S. Miller's experiments [24]. The first experiments on the modeling of non-equilibrium conditions with gas electric discharge simulating primary atmosphere and electrosynthesis of organic substances from anorganic ones under the energy of the electric field in a primary oxygen-free atmosphere were held in 1953 by S. Miller (USA) [24]. For this aim the mixture of water and gases consisted of hydrogen (H_2), methane (CH_4), ammonia (NH_3) and carbon monoxide (CO) was placed into a closed glass container being exposed by pulsating electrical spark discharges at the temperature of boiling water; oxygen was not allowed into the unit. After processing the reaction mixure by the electric discharge it was found that from the initial inorganic substance was synthesized organic compounds – aldehydes and amino acids. Experiments found that approximately ~10–15% of carbon was transferred into an organic form. However, about ~2% of carbon was detected in the amino acids, the most common of which was glycine. Initial analysis showed the presence in the reaction mixture obtained after the processing by spark electric discharge 5 amino acids. A more complete analysis carried out in 2008 [25], showed the formation by electrosynthesis in the reaction mixture 22 amino acids having from 5 to 20 carbon atoms in the molecule. Interestingly is that along with the amino acids in the reaction mixture after the treatment with electric spark discharges were detected trace amounts of nucleic acid precursors – nucleosides.

It should be noted that in the implementation of the gas discharge effect as well as in experiments of S. Miller are modeled extreme non-equilibrium conditions with gas electric discharge, resulting that in a thin layer of air gap with thickness ~100 μm are formed reactive radicals reacting with each other to form new compounds (electrosynthesis). Such extreme conditions are thought to have occurred in the primary oxygen-free atmosphere of the Earth, which

supposedly consisted of a mixture of water and gases – H_2, CH_4, NH_3 and CO, subjected to spark electrical discharges (lightning) under the conditions of high solar (UV) and geothermal activity.

The analogous experiment was conducted by the authors under laboratory conditions. According to our previous experiments, the first living structures may have evolved in warm and hot mineral water with a high content of bicarbonate (HCO_3^-) anions, cations of alkali metals (Na^+, Ca^{2+}, Mg^{2+}, Zn^{2+}) and deuterium in the form of HDO [26]. There occurred gas electric discharge (lightning) in the primordial atmosphere close to the water surface. In the course of experiment was used the similar gas electric discharge on water drops placed on the electrode of the device for gas electric discharge formation. The similar composition and water temperature were modeled on the electrode of the gas discharge device made of hostafan, with electric voltage – 15 kV, electric impulse duration – 10 μs; electric current frequency – 15 kHz, wherein the air gap layer on the boundary with water sample was formed the electrical discharge, similar to plasma phenomena (lightning) and the electrostatic discharge on the surface of organic and inorganic samples of various kinds. Water drops were heated up to the boiling point in an electric field of high frequency and the electric discharge was applied, analogious as that in the primordial atmosphere. As a result, an organized structure with a size of 1,2–1,4 mm was formed in interelectrode space (Fig. 7). It was formed as a result of accretion of smaller elementary structures sized up 5–10 μm into the biggest structure having the size 1,2–1,4 mm and concentrated in the spase where the electric field is applied.

It should be noted that no structure was organized in a control sample of water placed on the electrode. Before its placement on the electrode, the water was heated to boiling point and then cooled down. The structure organization increased with the increase of the duration of the gas electric discharge. Moreover, in experiments was observed the formation of small structures and their further “adjoining” to the larger structure. The large structure was preserved the original size for some time in the absence of the electric discharge.

Figure 7: The organized structure in water sample subjected to the temperature +100 °C in the electric field of high voltage and frequency (I. Ignatov, 2014). The material of the electrode – hostafan; the electric voltage – 15 kV, the electric impulse duration – 10 μs; the electric current frequency – 15 kHz.

This experiment shows that self-organization in water under certain external termal conditions may take place. In natural conditions water is heated up to +100 °C by the magma. The structure formed from heated water was evidently a result of self-organization. Living organisms are complex self-organizing systems. Thermodynamically they belong to the open systems because they constantly exchange substances and energy with the environment. The changes in the open systems are relatively stable in time. The stable correlation between components in an open system is called a dissipative structure. According to I. Prigozhin, the formation of dissipative structures and the elaboration to living cells is related to changes in entropy [27].

Taking into account these views it may be concluded that the initial stage of evolution, apparently, was connected with formation at high temperature of the mixtures of amino acids and nitrogenous substances – analogues of nucleic acids. Such synthesis is possible in aqueous solutions under thermal conditions in the presence of H_3PO_4. The next stage is polycondensation of amino acids into thermal proteinoids at temperatures 65–95 °C. After that in a mix of thermal proteinoids in hot water solutions were formed membrane like structures.

Our data are confirmed by experiments of T. Sugawara (Japan), who in 2011 created the membrane like proto cells from aqueous solution of organic molecules, DNA and synthetic enzymes under temperature close to the water boiling point +95 °C [28]. This data confirm the possibility that first organic forms of life originated in hot water.

IR-Spectroscopy of Water with Varying Content of Deuterium

Numerous studies carried out by us with various biological objects in D_2O, proved that when biological objects being exposed to water with different deuterium content, their reaction varies depending on the isotopic composition of water (the content of deuterium in water) and magnitude of isotope effects determined by the difference of constants of chemical reactions rates k_H/k_D in H_2O and D_2O. The maximum kinetic isotopic effect observed at ordinary temperatures in chemical reactions leading to rupture of bonds involving hydrogen and deuterium atoms lies in the range $k_H/k_D = 5–8$ for C–H versus C–D, N–D versus N–D, and O–D versus bonds [29].

The chemical structure of D_2O molecule is analogous to that one for H_2O, with small differences in the length of the covalent H–O-bonds and the angles between them. The molecular mass of D_2O exceeds on 10% that one for H_2O. The difference in nuclear masses stipulates the isotopic effects, which may be sufficiently essential for the $^1H/D$ pair. As a result, physical-chemical properties of D_2O differ from H_2O: D_2O boils at t = +101,44 °C, freezes at t = +3,82 °C, has maximal density at t =+11,2 °C (1,106 g/cm^3) [30]. In mixtures of ^2H_2O with H_2O the isotopic exchange occurs with high speed with the formation of semi-heavy water (^1HDO): $D_2O + H_2O = {}^1HDO$. For this reason deuterium presents in smaller content in aqueous solutions in form of ^1HDO, while in the higher content – in form of D_2O. The chemical reactions in D_2O are somehow slower compared to H_2O. D_2O is less ionized, the dissociation constant of D_2O is smaller, and the solubility of the organic and inorganic substances in D_2O is smaller compared to these ones in H_2O. Due to isotopic effects the hydrogen bonds with the participation of deuterium are slightly stronger than those ones formed of hydrogen.

The comparative analysis of IR-spectra of H_2O solutions and its deuterated analogues (D_2O, HDO) is of considerable interest for biophysical studies, because at changing of the atomic mass of hydrogen by deuterium atoms in H_2O molecule their interaction will also change, although the electronic structure of the molecule and its ability to form H-bonds, however, remains the same. The IR spectra of water usually contain three absorption bands, which can be identified as 1 – absorption band of the stretching vibration of OH^- group; 2 – absorption band of the first overtone of the bending vibration of the molecule HDO; 3 – absorption band of stretching vibration of OD^- group. OH^- group is able to absorb much infrared radiation in the infrared region of the IR-spectrum. Because of its polarity, these groups typically react with each other or with other polar groups to form intra-and intermolecular hydrogen bonds. The hydroxyl groups not involved in formation of hydrogen bonds are usually given the narrow bands in IR spectrum and the associated groups – broad intense absorption bands at lower frequencies. The magnitude of the frequency shift is determined by the strength of the hydrogen bond. Complication of the IR spectrum in the area of OH^- stretching vibrations can be explained by the existence of different types of associations, a manifestation of overtones and combination frequencies of OH^- groups in hydrogen

bonding, as well as the proton tunneling effect (on the relay mechanism. Such complexity makes it difficult to interpret the IR spectrum and partly explains the discrepancy in the literature available on this subject.

The local maximums in IR-spectra reflect vibrational-rotational transitions in the ground electronic state; the substitution with deuterium changes the vibrational-rotational transitions in H_2O molecule that is why it appears other local maximums in IR-spectra. In the water vapor state, the vibrations involve combinations of symmetric stretch ($\boldsymbol{\upsilon}_1$), asymmetric stretch ($\boldsymbol{\upsilon}_3$) and bending ($\boldsymbol{\upsilon}_2$) of the covalent bonds with absorption intensity (H_2O) $\boldsymbol{\upsilon}_1;\boldsymbol{\upsilon}_2;\boldsymbol{\upsilon}_3$ = 2671; 1178,4; 2787,7 cm^{-1}. For liquid water absorption bands are observed in other regions of the IR-spectrum, the most intense of which are located at 2100 cm^{-1} and 710–645 cm^{-1}. For D_2O molecule these ratio compiles 2723,7; 1403,5 and 3707,5 cm^{-1}, while for HDO molecule – 2671,6; 1178,4 and 2787,7 cm^{-1}. HDO (50 mole% H_2O + 50 mole% ^2H_2O; ~50 % HDO, ~25 % H_2O, ~25 % D_2O) has local maxima in IR-spectra at 3415 cm^{-1}, 2495 cm^{-1} 1850 cm^{-1} and 1450 cm^{-1} assigned to OH^- -stretch, OD^- -stretch, as well as combination of bending and libration and HDO bending respectively.

In the IR-spectrum of liquid water absorbance band considerably broadened and shifted relative to the corresponding bands in the spectrum of water vapor. Their position depends on the temperature [31]. The temperature dependence of individual spectral bands of liquid water is very complex. Furthermore, the complexity of the IR-spectrum in the area of OH^- stretching vibration can be explained by the existence of different types of H_2O associations, manifestation of overtones and composite frequencies of OH^- groups in the hydrogen bonds, and the tunneling effect of the proton (for relay mechanism). Such complexity makes it difficult to interpret the spectrum and partly explains the discrepancy in the literature available on this subject.

In liquid water and ice the IR-spectra are far more complex than those ones of the vapor due to vibrational overtones and combinations with librations (restricted rotations, i.g. rocking motions). These librations are due to the restrictions imposed by hydrogen bonding (minor L_1 band at 395,5 cm^{-1}; major L_2 band at 686,3 cm^{-1}; for liquid water at 0 ^oC, the absorbance of L_1 increasing with increasing temperature, while L_2 absorbance decreases but broadens with reduced wave number with increasing temperature [32]. The IR spectra of liquid water usually contain three absorbance bands, which can be identified on absorption band of the stretching vibration of OH^- group; absorption band of the first overtone of the bending vibration of the molecule HDO and absorption band of stretching vibration of OD^- group. Hydroxyl group OH^- is able to absorb much infrared radiation in the infrared region of the IR-spectrum. Because of its polarity, these groups typically react with each other or with other polar groups to form intra- and inter-molecular hydrogen bonds. The hydroxyl groups, which are not involved in formation of hydrogen bonds, usually produce the narrow bands in IR spectrum, while the associated groups – broad intense absorbance bands at lower frequencies. The magnitude of the frequency shift is determined by the strength of the hydrogen bond. Complication of the IR spectrum in the area of OH^- stretching vibrations can be explained by the existence of different types of associations of H_2O molecules, a manifestation of overtones and combination frequencies of OH^- groups in hydrogen bonding, as well as the proton tunneling effect (on the relay mechanism).

Assignment of main absorbtion bands in the IR-spectrum of liquid water is given in Table 2. The IR spectrum of H_2O molecule was examined in detail from the microwave till the middle (4–17500 cm^{-1}) visible region and the ultraviolet region – from 200 nm^{-1} to ionization limit at 98 nm^{-1} [33]. In the middle visible region at 4–7500 cm^{-1} are located rotational spectrum and the bands corresponding to the vibrational-rotational transitions in the ground electronic state. In the ultraviolet region (from 200 nm^{-1} to 98 nm^{-1}) are located bands corresponding to transitions from the excited electronic states close to the ionization limit in the electronic ground state. The intermediate region of the IR-spectrum – from 570 nm to 200 nm corresponds to transitions to higher vibrational levels of the ground electronic state.

Table 2: The assignment of main frequencies in IR-spectra of liquid water H_2O and D_2O

Main vibrations of liquid H_2O and ^2H_2O				
Vibration(s)	**H_2O (t = 25 °C)**		**D_2O (t = 25 °C)**	
	υ, cm^{-1}	**E_0, M^{-1} cm^{-1}**	**υ, cm^{-1}**	**E_0, M^{-1} cm^{-1}**
Spinning ν_1 + deformation ν_2	780–1645	21,65	1210	17,10
Composite $\nu_1 + \nu_2$	2150	3,46	1555	1,88
Valence symmetrical ν_1, valence asymmetrical ν_3, and overtone $2\nu_2$	3290–3450	100,65	2510	69,70

Results of IR-spectroscopy with Infra Spec VFA-IR device show that at λ = 4,1 μm, even at low concentrations of deuterium of 0,35 and 0,71%, there is observed a decline in the local maximums relative to the local maximum of 100% pure water (the local maximums in IR-spectra reflect vibrational-rotational transitions in the ground electronic state because at changing the atomic mass of hydrogen and deuterium atoms in the water molecule their interaction will also change, although the electronic structure of the molecule and its ability to form H-bonds, however, remains the same; with the substitution with deuterium the vibrational-rotational transitions are changed, that is why it appears other local maximums in IR-spectra. These results are shown in Figure 9. The result is reliable regarding the content of deuterium in natural waters from 0,015–0,03%.

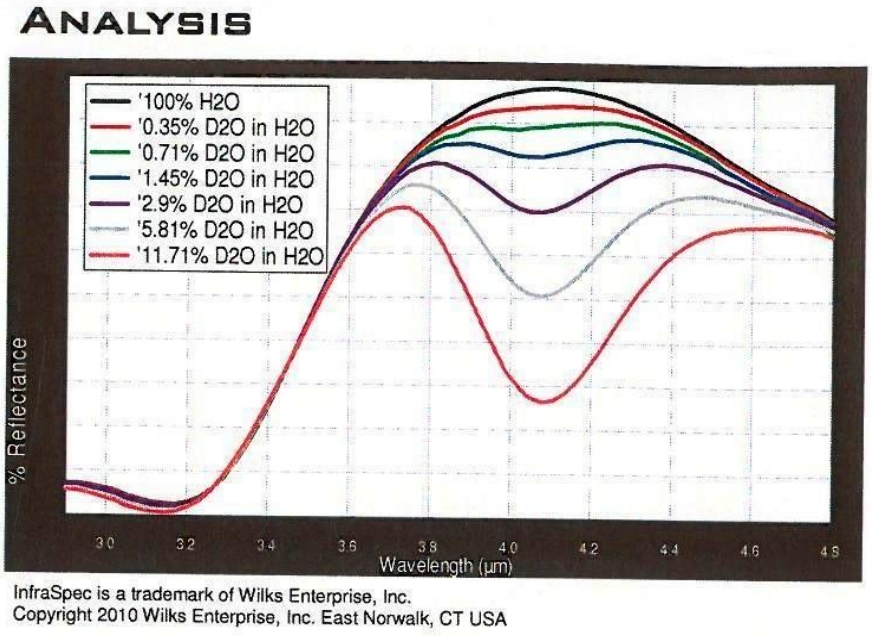

Figure 9: The typical IR-spectra of water with varying content of deuterium

At further transition from H_2O monomers to H_4O_2 dimmer and H_6O_3 trimmer absorption maximum of valent stretching vibrations of the O–H bond is shifted toward lower frequencies ($\boldsymbol{\upsilon}_3$ = 3490 cm^{-1} and $\boldsymbol{\upsilon}_1$ = 3280 cm^{-1}) [34] and the bending frequency increased ($\boldsymbol{\upsilon}_2$ = 1644 cm^{-1}) because

of the hydrogen bonding. The increased strength of hydrogen bonding typically shifts the stretch vibration to lower frequencies (red-shift) with greatly increased intensity in the infrared due to the increased dipoles. In contrast, for the deformation vibrations of the H–O–H, it is observed a shift towards higher frequencies. Absorption bands at 3546 and 3691 cm^{-1} were attributed to the stretching modes of the dimmer [$(H_2O)_2$]. These frequencies are significantly lower than the valence modes of ν_1 and ν_3 vibrations of isolated H_2O molecules at 3657 and 3756 cm^{-1} respectively). The absorption band at 3250 cm^{-1} represents overtones of deformation vibrations. Among the frequencies between 3250 and 3420 cm^{-1} it is possible the Fermi resonance (this resonance is a single substitution of intensity of one fluctuation by another fluctuation when they accidentally overlap each other). The absorption band at 1620 cm^{-1} is attributed to the deformation mode of the dimmer. This frequency is slightly higher than the deformation mode of the isolated H_2O molecule (1596 cm^{-1}). A shift of the band of deformation vibration of water in the direction of high frequencies at the transition from a liquid to a solid state is attributed by the appearance of additional force, preventing O–H bond bending. The deformation absorption band in IR-spectrum of water has a frequency at 1645 cm^{-1} and very weak temperature dependence. It changes little in the transition to the individual H_2O molecule at a frequency of 1595 cm^{-1}. This frequency is found to be sufficiently stable, while all other frequencies are greatly affected by temperature changes, the dissolution of the salts and phase transitions. It is believed that the persistence of deformation oscillations is stipulated by processes of intermolecular interactions, e.g. by the change in bond angle as a result of interaction of H_2O molecules with each other, as well as with cations and anions.

Thus, the study of the characteristics of the IR spectrum of water allows to answer the question not only on the physical parameters of the molecule and the covalent bonds at isotopic substitution with deuterium, but also to make a certain conclusion on associative environment in water. The latter fact is important in the study of structural and functional properties of water associates and its isotopomers at the isotopic substitution with deuterium. T**he substitution of H with D affects the stability and geometry of hydrogen bonds in an apparently rather complex way and may through the changes in the hydrogen bond zero-point vibration energies, alter the conformational dynamics of hydrogen (deuterium)-bonded structures of macromolecules as DNA and proteins in D_2O.**

Conclusion

The data obtained testify that origination of first organic forms of life depends on physical-chemical properties of water and external factors – temperature, pH, electric discharges and isotopic composition. Hot mineral alkaline water interacting with $CaCO_3$ is most closed to these conditions. Next in line with regard to its quality is seawater. For chemical reaction of dehydration-condensation to occure in hot mineral water, water is required to be alkaline with the pH ranged 9–11. In warm and hot mineral waters the local maximums in IR-spectra from 8 to 14 μm were more expressed in comparison with the local maximums measured in the same water samples with lower temperature. The content of deuterium in hot mineral water may be increased due to the physical chemical processes of the deuterium accumulation stipulated by the solar radiation, volcanic geothermal processes and electric discharges in the atmosphere. These natural processes could lead to the enrichment of the hydrosphere by deuterium in the form of HDO which evaporates more slowly than H_2O, but condenses faster. If the primary hydrosphere really contained HDO, that this may explain the thermal stability of the first organic life forms in the hot mineral water, as the thermal stability of deuterated macromolecules like DNA and proteins in D_2O solutions is somewhat higher than their protonated forms due to isotopic effects of deuterium.

Acknowledgements

The authors wish to thank M. Chakarova from Bulgarian Academy of Sciences for registering IR-spectra.

References:

1. Ignatov I. Color coronal (Kirlian) spectral analysis in modeling of nonequilibrioum conditions with the gas electric discharges simulating primary atmosphere. S. Miller's experiments

/ I. Ignatov, O.V. Mosin // Naukovedenie. 2013. № 3(16). P. 1–15 [in Russian] [Online] Available: URL: http://naukovedenie.ru/PDF/05tvn313.pdf (May 10, 2013).

2. Ignatov I. Isotopic composition of water and its temperature in the evolutionary origin of life and living matter / I. Ignatov, O.V. Mosin // Naukovedenie. 2013. № 1(14). P. 1–16 [in Russian] [Online] Available: URL: http://naukovedenie.ru/PDF/42tvn113.pdf (February 13, 2013).

3. Ignatov I. Possible processes for origin of life and living matter with modeling of physiological processes of bacterium *Basillus subtilis* as model system in heavy water / I. Ignatov, O.V. Mosin // Journal of Natural Sciences Research. 2013. V. 3, № 9. P. 65–76.

4. Ignatov I. Isotopic composition of water and its temperature in modeling of primordial hydrosphere experiments / I. Ignatov, O.V. Mosin. Euro-Eco, Hanover. 2012. P. 62.

5. Linsky J.L. D/H and nearby interstellar cloud structures / Ed. J.I. Linsky. Space Science Reviews, NY: Springer Science, Business Media. 2007. V. 130. 367 p.

6. Ignatov I. Which water is optimal for the origin (generation) of life? / I. Ignatov. – Euromedica, Hanover. 2010. P. 34–37.

7. Ignatov I. Modeling of possible processes for origin of life and living matter in hot mineral and seawater with deuterium / I. Ignatov, O.V. Mosin // Journal of Environment and Earth Science. 2013. V. 3, № 14. P. 103–118.

8. Szostak J.W. An optimal degree of physical and chemical heterogeneity for the origin of life? / J.W. Szostak // Philos. Trans. Royal Soc. Lond. Biol. Sci. 2011. Vol. 366, № 1580. P. 2894–901.

9. Mulkidjanian A.Y. On the origin of life in the Zinc world. Validation of the hypothesis on the photosynthesizing zinc sulfide edifices as cradles of life on Earth / A.Y. Mulkidjanian, M.Y. Galperin // Biology Direct. 2009. V. 4. P. 26.

10. Trevors J.I. Hypothesis: origin of live in hydrogel environment / J.I. Trevors, G.H. Pollack // Progress in biophysics and molecular biology. 205. V. 89, № 1. P. 1–8.

11. Ignatov I. Origin of life and living matter in hot mineral water. Conference on the Physics, Chemistry and Biology of Water, Vermont Photonics, USA. 2012. P. 67.

12. Ignatov I. Method for colour coronal (Kirlian) spectral analysis // I. Ignatov, O.V. Mosin // Biomedical Radio electronics. 2013. V. 1. P. 38–47 [in Russian].

13. Schirber M. First fossil-makers in hot water / M. Schirber M. // Astrobiology magazine. 2010 [Online] Available: URL: http://www.astrobio.net/exclusive/3418/first-fossil-makers-in-hot-water (January 3, 2010).

14. Ponsa M.L. Early archean serpentine mud volcanoes at Isua, Greenland, as a niche for early life / M.L. Pons, G. Quitte, T. Fujii, M.T. Rosingc, B. Reynarda, F. Moynierd, Ch. Doucheta, F. Albaredea // Proc. Natl. Acad. Sci. U.S. 2011. V. 108. P. 17639–17643.

15. Kurihara K. Self-Reproduction of supramolecular giant vesicles combined with the amplification of encapsulated DNA / K. Kurihara, M. Tamura, K. Shohda, T. Toyota, K. Suzuki, T. Sugawara // Nature Chemistry. 2011. V. 4, № 10. P. 775–781.

16. Calvin M. Chemical evolution / Ed. M. Calvin. Oxford: Clarendon. 1969. 278 p.

17. Mathews C.N. Peptide synthesis from hydrogen-cyanide and water / C.N. Mathews, R. Moser // Nature. 1968. Vol. 215. P. 1230–1234.

18. Miller S.L. A production of amino acids under possible primitive Earth conditions / S.L. Miller // Science. 1953. V. 117, № 3046. P. 528–529.

19. Abelson P. Chemical events on the "primitive" earth / P. Abelson // Proc. Natl. Acad. Sci. U.S. 1966. V. 55. P. 1365–1372.

20. Harada I. Thermal synthesis of natural ammo-acids from a postulated primitive terrestrial atmosphere / I. Harada, S.W. Fox, S.W. // Nature. 1964. V. 201. P. 335–336.

21. Fox S.W. Catalytic decomposition of glucose in aqueous solution by thermal proteinoids / S.W. Fox, G. Krampitz // Nature. 1964. V. 203. P. 1362–1364.

22. Fox S.W. Melanocytestimulating hormone: Activity in thermal polymers of alpha-ammo acids / S.W. Fox, C.T. Wang // Science. 1968. V. 160. P. 547–548.

23. Nakashima T. Metabolism of proteinoid microspheres / Ed. T. Nakashima. In: Origins of life and evolution of biospheres. 1987. V. 20, № (3–4). P. 269–277.

24. Miller S.L. A production of amino acids under possible primitive Earth conditions // Science. 1953. Vol. 117, № 3046. P. 528–529.

25. Johnson A.P., Cleaves H.J., Dworkin J.P., Glavin D.P., Lazcano A., Bada J.L. The Miller volcanic spark discharge experiment // Science. 2008. V. 322. № 5900. P. 404–412.

26. Ignatov I., Mosin O.V. Color coronal (Kirlian) spectral analysis in modeling of nonequilibrioum conditions with the gas electric discharges simulating primary atmosphere. S. Miller's experiments / I. Ignatov, O.V. Mosin // *Naukovedenie. 2013. Vol.* 3, № 16. P. 1–15 [in Russian] [Online] Available: URL: http://naukovedenie.ru/PDF/05tvn313.pdf (May 10, 2013).

27. Nikolis P. Self-organization in non-equilibrium systems / Ed. P. Nikolis, I. Prigozhin. – Moscow: Mir. 1979. P. 1–512 [in Russian].

28. Sugawara T. Self-reproduction of supramolecular giant vesicles combined with the amplification of encapsulated DNA / T. Sugawara // Nature Chemistry. 2011. V. 1127. P. 775–780.

29. Mosin O.V. Studying of isotopic effects of heavy water in biological systems on example of prokaryotic and eukaryotic cells / O.V. Mosin, I. Ignatov // Biomedicine, Moscow. 2013. V. 1, № 1–3. P. 31–50 [in Russian].

30. Mosin O.V. Studying of methods of biotechnological preparation of proteins, amino acids and nucleosides, labeled with stable isotopes ^{2}H and ^{13}C with high levels of isotopic enrichment / O.V. Mosin. Autoref. disser. thesis PhD. – Moscow: M.V. Lomonosov State Academy of Fine Chemical Technology, 1996. 26 p.

31. Ignatov I. Modeling of possible processes for origin of life and living matter in hot mineral and seawater with deuterium / I. Ignatov, O.V. Mosin. Journal of Environment and Earth Science. 2013. *V.* 3, № 14. P. 103-118.

32. Zelsmann H.R. Temperature dependence of the optical constants for liquid H_2O and D_2O in the far IR region / H.R. Zelsmann **// *J. Mol. Struct. 1995. V.*** 350. P. 95–114.

33. Yakhnevitch G.B. Infrared spectroscopy of water / G.B. Yakhnevitch. – Moscow: Nauka, 1973. 207 p. [in Russian].

34. Ignatov I. Structural mathematical models describing water clusters / I. Igantov, O.V. Mosin // Journal of Mathematical Theory and Modeling. 2013. V. 3. № 11. P. 72-87.

УДК 735.29: 573.552

Исследование гидрологических условий происхождения органических форм жизни в горячей минеральной воде с HDO

[1] Игнат Игнатов
[2] Олег Викторович Мосин

[1] Научно-исследовательский центр медицинской биофизики (РИЦМБ), Болгария
Профессор, доктор наук Европейской академии естественных наук (ФРГ), директор НИЦМБ.
1111, София, ул. Н. Коперника, 32/6
mbioph@dir.bg
[2] Московский государственный университет прикладной биотехнологии, Российская федерация
Старший научный сотрудник кафедры биотехнологии, канд. хим. наук.
103316, Москва, ул. Талалихина, 33
E-mail: mosin-oleg@yandex.ru

Аннотация

Изучен состав воды, температура и значение pH в экспериментах по моделированию первичной гидросферы и возможных условий возникновения органических форм жизни в горячей минеральной воде с HDO. Для этой цели проведены исследования горячей минеральной и морской воды из Болгарских источников методами ИК- и ДНЭС-спектроскопии. В качестве модельных систем использовали сок кактуса *Echinopsis pachanoi* и средиземноморскую медузу *Cotylorhiza tuberculata*. Рассмотрены реакции конденсации-дегидратации в щелочных водных растворах со значением pH = 9–10, результатом которых является синтез из мелких молекул более крупных органических молекул полимеров как короткие полипептиды, а также механизмы аккумуляции дейтерия в форме HDO в горячей

минеральной воде. Показано, что горячие минеральные воды с температурой от +65 °С до +95 °С и значением pH от 9 до 11 более пригодны для возникновения жизни, чем другие исследованные образцы воды. В горячей минеральной воде локальные максимумы в ИК-спектре проявлялись больше всего, по сравнению с локальными максимумами в ИК-спектре той же воды при более низкой температуре. Разница в локальных максимумах от +20 °С до +95 °С при увеличении температуры на каждый +5 °С составила в соответствии с *t*-критерием Стьюдента $p < 0,05$.

Ключевые слова: дейтерий, гидросфера, эволюция, возникновение жизни, ИК-спектроскопия, ДНЭС.

Published in the Russian Federation
European Journal of Molecular Biotechnology
Has been issued since 2013.
ISSN: 2310-6255
E-ISSN: 2409-1332
Vol. 10, Is. 4, pp. 228-240, 2015

DOI: 10.13187/ejmb.2015.10.228
www.ejournal8.com

UDC 57.089.67 : 616.314-089

Molecular Approaches to Functionalization of Dental Implant Surfaces

Angelina O. Zekiy

First Moscow Medical University, Russian Federation
Trubetzkaya St., 8, Bd. 2, 119991 Moscow
PhD in Medicine, Associate Professor
E-mail: angelinaolegovna@gmail.com

Abstract

The present review examines several approaches to improve properties of dental implants by modifying their bioactive surfaces (functionalization) using the techniques of molecular transplantation. The first group of functional ligands is designed to enhance osseointegration of implants, it includes growth factors, promoting the formation and bone remodeling: bone morphogenetic proteins (BMPs), platelet-derived growth factor (PDGF), fibroblast growth factor (FGF) and their combinations with each other, and several other ones. The second group of bioactive molecules does not directly stimulate bone formation, but it promotes osteoblast seeding on the implant surface due to the adhesive properties, thus accelerating osseointegration. Finally, the third group of substances used to increase the antibacterial properties of coatings, thereby reducing the formation of bacterial film on the implant surface and the risk of inflammatory rejection of the implant. Key issues of using biofunctional coatings, despite their obvious promise today still are relatively high cost, difficulties of controlling properties and its storage between the fabrication and installation of implants in the bone of the recipient.

Keywords: dental implantation, functional coating, bioactive surface, cellular adhesion, osseointegration, platelet-derived growth factors, bone morphogenetic proteins.

Introduction

The success of prosthetic dentistry, due to the advent of new diagnostic and therapeutic technologies have led to the fact that dental implantation claims to be a "gold standard" in the restoration after lost of teeth. The number of operations in leading dental clinics in the thousands per year with efficiency of over 95 %, and in some age groups of the urban population in developed nations, the part of people with dental implants is approaching to 20 % [16, 56].

The long-run objective of dental implantation is a stable recovery of function of dental system by restoring the three-dimensional dental occlusion, which is unconceivable without the formation of a strong bond between the implant and the recipient bone, osseointegration [2, 21, 37, 40, 57]. The failures of dental implantation specifically associated with a partial loss of foregoing connection, with bacterial population of the resulting gaps and with inflammation of surrounding tissues [49, 55].

The surface of the metal structures installed in bone tissue is continuously improves. This is one of the main approaches to solving the defined problem. Ideally, it should be absolutely biocompatible, have a high specific area and cause intensive bone tissue formation, that is, have osteoinductive effect [1, 8, 22]. The number of foreign analytical reviews [7, 44, 58] describes ways to enhance osseointegration by creating biomimetic micro-relief surfaces and by coating implants of various materials with osteoinductive properties.

Although the number of such modifications is theoretically infinite (calculated in the hundreds in practice), manufacturers seem to reach the limit improving the osseointegration by these methods. This is evident from the fact that there are no proven advantages of modified surfaces over conventional screw implants in a few clinical trials [61, 62].

The surface functionalization usage opens fundamentally different possibilities. The idea is to use them in a controlled placement on the implant' surface of active molecules with biological effect - adhesion, growth factors, etc., which allows the quickest possible osteogenesis initialization throughout the implant surface. Making the surface of the predefined useful health properties (functionalization) is achieved in this case by molecular transplantation [3, 52]. This review is devoted to observe the advantages and unresolved problems of this approach.

1. Functionalization with growth factors

The main purpose of the active biomolecules placement on the implant surface concludes in diminishing the initial inflammatory response to installation of the implant due to their gradual release into the tissue. Most intensive bone formation and reduction of surface colonization by microorganisms resulted from this action. Some growth factors and fragments of the organic matrix of bone, known biologically active peptides, are suitable on the role of these substances [23, 30].

In the detailed review I. Nishimura [41] described two dozen growth factors somehow involved in osteogenesis. Nevertheless, at the moment only four growth factors are promising for the needs of implantology: bone morphogenetic proteins (BMP-2 and BMP-7), fibroblast growth factor (FGF-2) and platelet-derived growth factor (PDGF-B). Common functional scheme of molecular interactions in system 'implant – bone' presented in Figure.

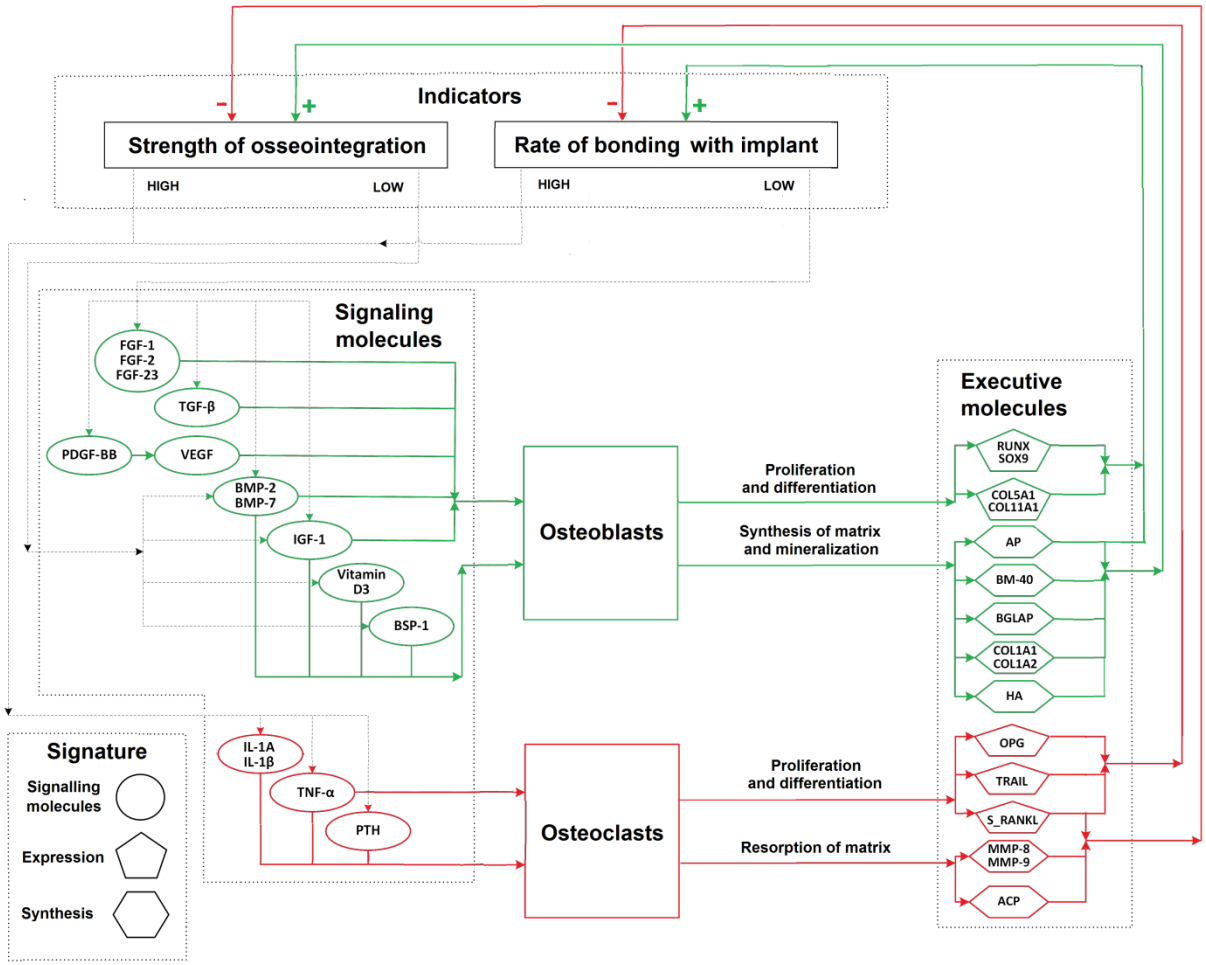

Figure. The functional system 'implant – bone' can be subdivided into three blocks. Signaling molecules form the block (I) managing the activity of the two cell populations, osteoblasts and osteoclasts. Synthesis and/or expression of executive molecules (II) reflect functional activity of these cells. A set of indicators the two final characteristics of osseointegration, such as the formation and the strength of the bond between the implant and the bone (III), can influence the concentration of signaling molecules through feedback.

Transforming growth factor (TGF-β) strongly accelerating the division and differentiation of many types of mesenchymal cells, was ineffective in these conditions, because of the considerable chondroinductive effect that could not secure the stability of implant engraftment [4]. Insulin-like growth factor (IGF-1 and IGF-2) and vascular growth factor (VEGF) have been effective only in combination with the above factors. Essentials facts about the main growth factors currently used to stimulate the osseointegration of dental implants are summarized in Table.

Table

Growth factors and biologically active peptides used for molecular transplantation due to fabrication of dental implants (on clinical trial stage)

Molecules	Mechanism of action	Ref.
Alone growth factors		
BMP-2 BMP-7	Cell differentiation and stimulation of osteogenesis	[6, 11, 14, 32, 33]
FGF-2	Mitogenesis and suppression of apoptosis in osteogenic cell population	[25, 35]

PDGF-B	Mitogenesis and chemotaxis of mesenchymal and osteogenic cells	[10, 17, 43]
Combinations of growth factors		
PDGF-B + IGF-1	Additional stimulation of osteogenesis and collagen synthesis	[45]
BMP-2 + VEGF	Additional stimulation of osteogenic differentiation and mineralization of matrix	[24, 34, 47]
BMP-2 + FGF-2	Additional stabilization of osteoblast proliferation	[29, 38]
BMP-2 + TGF-β	Most intensive production of bone matrix	[54]
Adhesive and antibacterial peptides		
RGD YIGSR REDV	Most intensive adhesion of matrix proteins to implant surface	[18, 36, 52]
GL13K	Protection of implant surface to bacterial colonization	[18, 64]

Among the BMPs belonging to the TGF-β superfamily are the most relevant for dental implantology BMP-2 and BMP-7 isoforms, which proved all the effects of bone formation stimulation *in vivo* [4, 39]. Recently a group of Russian scientists has been developed the original method of producing recombinant human BMP-2 (rhBMP-2) with a high-producing strain based on *Escherichia coli*. On the basis of rhBMP-2 the osteoplastic material «Gamalant™ - pasta Forte Plus" is created. It has high osteoinductive and effectively influence on the process of reparative osteogenesis [11]. To ensure the growth factor delivery in the osseointegration area, the BMP is applied to the surface of the implant in the form of a polymer-containing gel or emulsion of a polyelectrolyte rate of approximately 200 micrograms per one product [14, 31, 65].

Recombinant FGF-2 which increases the number of functional osteoblasts successfully used in the clinic for the augmentation of the dental arch in patients with periodontitis [25]. It is contemplated to be a osteoregeneration stimulator when dental implants are installed, but is more effective against soft tissue contacting with the cervix of the implant [35].

Platelet-derived growth factor (PDGF-B) is a potent mitogen and chemotactic agent for a variety of mesenchymal cells, including osteoblasts, and therefore its isolated usage, as expected, will have a certain effect [17]. Recently, Chang et al. [7] have demonstrated for PDGF to be able stimulating osseointegration of dental implants *in vivo*. On the other hand, it has been reported that the isolated recombinant PDGF affects bone formation adversely [27]. The successful attempt to transfer gene *pdgfb* to bone marrow mesenchymal stem cells has been reported [10], but their osteoinductive effect was shown only in rats at volume replacement of bone defects with collagen-based scaffolds.

In clinics the use of platelet-rich plasma or platelet-fibrin clot may be an equivalent of pure PDGF usage. This material comprises a mixture of biologically active substances include growth factors, and the PDGF prevails therein. This method is gaining popularity due to safety and the possibility of using autologous source of growth factors ex tempore, and it shows good results in a number of clinical studies [20, 28].

The presence of multiple growth factors involved in bone formation, has pushed developers to attempts to use them as combinations with complementary effects. Successful combinations are given in Table 1.

2. Usage of biologically active peptides

Proteins of extracellular bone matrix are logical candidates for molecular transplantation. Currently, functional coatings made with the inclusion of fibronectin, laminin and vitronectin were fabricated [1, 12]. Thus, metal processing with fibronectin stimulating osteoblasts differentiation and tissue mineralization, contributed to strong osseointegration of implants in experimental models in vivo [48].

Recently, the focus has shifted to the usage of functional domains consisting of only a few amino acids of the necessary protein because it does not require control of the bioactive group

spatial accessibility. Arg-Gly-Asp (RGD), the adhesive domain derived from fibronectin and laminin, is the most successful example of biologically active peptide [36, 52]. Other sequences, such as Tyr-Ile-Gly-Ser-Arg (YIGSR), or Arg-Glu-Asp-Val (REDV), can also accelerate osseointegration. Some modifications with covalent peptides binding with coating before the anode deposition are the most stable [5, 52].

It is known the attempt to include in the coating one of the bisphosphonates (alendronate), which was able to block fibrogenesis in favor of bone formation. This effect was confirmed at the culture of mesenchymal stem cells seeded onto titanium with a functional coating [19]. Also using cell cultures L. Russo et al. [50] showed anchor proteins, which were necessary to start a full osseointegration, to increase adhesion after raising the number of free amino groups on the implant surface by reacting HA carbonate with (3-aminopropyl)-trietoksylane.

Some osteoinductive biopolymers, in particular chitosan, are also treated as the substrate coating. The material has adequate wettability and bioresorption degree. It is capable of inducing osteogenesis on osteoblast culture [46]. The experiment shows the positive effect of chitosan surface modification of titanium implants. When titanium implants with bioactive porous surface and additional fine chitosan coating were installed, the bone formation round them accelerated and become more intensive in conjunction with morphological markers of strong remodeling and sealing the surrounding bone [42].

Common problems associated with the use of growth factors and biologically active peptides can be reduced to implants cost increase, complications with the usage and preservation of the bioactive material before implantation, and with the insufficiently developed questions of kinetics and topography of their releasing in tissues around the implant, due to combined application, in particular - [23, 52]. Apparently, to date, this approach has not yet been able to compete with varying materials and relief of implants.

3. Antibacterial coating

There are several ways to functionalize the coatings that can be used to significant improvement the durability and osseointegration of the implant in the body. One of them is to enhance antibacterial properties, since infection is the second most common cause of implant failure [53, 60].

In this role, silver ions are the most studied and close to implementation) [9, 13]. Particles of gold, copper, zinc, SeO_3^-, strontium, cerium, gallium, and a number of more exotic rare earth metals are also could be potential agents. A number of their potentially useful features are summarized in a review [26], but it is unlikely that they have near-term clinical applications because of significant rise the coatings costs.

On the basis of the concept of the surfaces antibacterial properties, K.V. Holmberg et al. [18] developed coating with GL13K peptide inclusion. Such peptide had been derived from the soluble protein fraction of the parotid gland. As a coating it showed a high bacteriostatic activity against *Porphyromonas gingivalis,* which is the main microorganism associated with peri-implant pathology. While all the required properties of the implant surface were providing: high hydrophobicity (1), mechanical and thermal stability (2), resistance to enzymatic degradation (3), and high osteoinductive effect (4). The coating was recommended for clinical trials.

In a clinical study H. Tsuchiya et al. [59] used commercial dental implants with original iodine-containing coating in 158 patients with a high risk of postoperative infection. During the year complications occurred in 3 of 158 cases in main group, and in all 64 cases of implantation without the iodine-containing coating usage.

Although most of the work supports the idea that the functionalization of the implant surface can improve and accelerate its osseointegration, the key to the commercial success of this approach (besides the absolute clench the matter of cost) is to adapt the proposed methods to the surfaces of the specific dental alloys and to conserve controlled surface properties over the time between the manufacturing and implantation.

Conclusion

The surface functionalization by dynamically related ligands, possessing adhesive, modulating cell phenotype and/or antibacterial properties, at least at the level of the preclinical and first clinical trial, demonstrates the ability to improve the dental implants osseointegration.

Apparently, controlled surface nanoscale modification of two-dimensional (nanopatterns) and one-dimensional nature (nano-pores and nano-columns) is promising approach. The key issue, given the almost infinite possibilities of variation, is to reveal patterns of correlation between the composition, surface' fine-texture and the expected biomechanical properties of the implant, the overall dynamics of osseointegration.

Acknowledgements

The author thanks A.A. Shyrokiy for the help in the description of molecular processes in the area of osseointegration in terms of bio-Cybernetics and the drafting of the relevant scheme.

References:

1. Albertini M., Fernandez-Yague M., Lázaro P., et al. (2015) Advances in surfaces and osseointegration in implantology. Biomimetic surfaces. *Med. Oral Patol. Oral Cir. Bucal.* 20(3), e316–e325.

2. Bassi F., Carr A.B., Chang T.L., et al. (2013) Clinical outcomes measures for assessment of longevity in the dental implant literature: ORONet approach. *Int. J. Prosthodont.* 26(4), pp. 323-330.

3. Berglundh T., Giannobile W.V. (2013) Investigational clinical research in implant dentistry: beyond observational and descriptive studies. *J. Dent. Res.* 92(12 Suppl), pp. 107S–108S.

4. Bessa P.C., Casal M., Reis R.L. (2008) Bone morphogenetic proteins in tissue engineering: the road from the laboratory to the clinic, part II (BMP delivery). *J. Tissue Eng. Regen. Med.* 2(2-3), pp. 81-96.

5. Beutner R., Michael J., Schwenzer B., Scharnweber D. (2010) Biological nano-functionalization of titanium-based biomaterial surfaces: a flexible toolbox. *J. Royal Soc. Interface.* 7, pp. S93–S105.

6. Casap N., Laviv A., Debecco M., et al. (2015) Imperforate titanium shell enclosing recombinant human bone morphogenetic protein-2-induced bone formation for high-profile dental implants in rabbit tibia. J. Oral Maxillofac. Surg. 73(2), pp. 245-252.

7. Chang P.-C., Lang N.P., Giannobile W.V. (2010) Evaluation of functional dynamics during osseointegration and regeneration associated with oral implants: a review. *Clin. Oral Implants Res.* 21(1), pp. 1–12.

8. Coelho P.G., Granjeiro J.M., Romanos G.E., et al. (2009) Basic research methods and current trends of dental implant surfaces. *J. Biomed. Mater. Res. B. Appl. Biomater.* 88(2), pp. 579–596.

9. Corrêa J.M., Mori M., Sanches H.L., et al. (2015) Silver nanoparticles in dental biomaterials. *Int. J. Biomater. 2015.* e485275.

10. Elangovan S., D'Mello S.R., Hong L., et al. (2014) The enhancement of bone regeneration by gene activated matrix encoding for platelet derived growth factor. *Biomater.* 2014; 35(2), pp. 10-15.

11. Fedorova M.Z., Nadezhdin S.V., Semikhin A.S., et al. (2011) [Experimental estimation of composite material containing The protein-mineral components and recombinant bone morphogenetic protein-2 as a covering of titanium implants] [Traumatology and orthopedics of Russia*] Travmatologiya i ortopediya Rossii.* 2(60), pp. 101-106.

12. Gao X., Zhang X., Song J., et al. Osteoinductive peptide-functionalized nanofibers with highly ordered structure as biomimetic scaffolds for bone tissue engineering Int. J. Nanomedicine. 10, pp. 7109–7128.

13. González-Sánchez M.I., Perni S., Tommasi G., et al. (2015) Silver nanoparticle based antibacterial methacrylate hydrogels potential for bone graft applications. *Mater. Sci. Eng. C. Mater. Biol. Appl.* 50, pp. 332–340.

14. Guillot R., Gilde F., Becquart P., et al. (2013) The stability of BMP loaded polyelectrolyte multilayer coatings on titanium. *Biomater.* 34(23), pp. 5737–5746.

15. Gupta G. (2012) Gingival crevicular fluid as a periodontal diagnostic indicator- I: Host derived enzymes and tissue breakdown products. *J. Med. Life.* 5(4), pp. 390–397.

16. Harford J. (2009) Population ageing and dental care. *Com. Dent. Oral Epidemiol.* 37(2). P. 97-103.

17. Hollinger J.O., Hart C.E., Hirsch S.N., et al. (2008) Recombinant human platelet-derived growth factor: biology and clinical applications. *J. Bone Joint Surg. Amer.* 90 (Suppl 1), pp. 48–54.

18. Holmberg K.V., Abdolhosseini M., Li Y., et al. (2013) Bio-inspired stable antimicrobial peptide coatings for dental applications. *Acta Biomater.* 9(9), pp. 8224–8231.

19. Hu X., Neoh K.G., Shi Z., et al. (2013) An i*n vitro* assessment of fibroblast and osteoblast response to alendronate-modified titanium and the potential for decreasing fibrous encapsulation. *Tissue Eng. Pt A.* 19(17-18), pp. 1919–1930.

20. Inchingolo F., Ballini A., Cagiano R., et al. (2015) Immediately loaded dental implants bioactivated with platelet-rich plasma (PRP) placed in maxillary and mandibular region. *Clin. Ter.* 166(3), pp. 146-152.

21. Jang H.W., Kang J.K., Lee K., et al. (2011) A retrospective study on related factors affecting the survival rate of dental implants. *J. Adv. Prosthodont.* 3(4), pp. 204-215.

22. Kalita V.I., Malanin D.A., Mamaeva V.A., et al. (2009) [Modification of intraosseal implants surfaces: current research and nanotechnologies] *[J. Volgograd State Med. Univ.] Vestnik Volgogradskogo Gosudarstvennogo Meditzinskogo Universiteta.* (4), pp. 17–22. [in Russ.].

23. King W.J., Krebsbach P.H. (2012) Growth factor delivery: How surface interactions modulate release in vitro and in vivo. *Adv. Drug Deliv. Rev.* 64(12), pp. 1239–1256.

24. Kempen D.H., Lu L., Heijink A., et al. (2009) Effect of local sequential VEGF and BMP-2 delivery on ectopic and orthotopic bone regeneration. *Biomater.* 30: 2816–2825.

25. Kitamura M., Nakashima K., Kowashi Y., et al. (2008) Periodontal tissue regeneration using fibroblast growth factor-2: randomized controlled phase II clinical trial. *PLoS ONE.* 3, e2611.

26. Kolmas J., Groszyk E., Kwiatkowska-Różycka D. (2014) Substituted hydroxyapatites with antibacterial properties. *Biomed. Res. Int. 2014.* e178123.

27. Kono S.J., Oshima Y., Hoshi K., et al. (2007) Erk pathways negatively regulate matrix mineralization. *Bone.* 40(1), pp. 68–74.

28. Kundu R., Rathee M. (2014) Effect of platelet-rich-plasma (PRP) and implant surface topography on implant stability and bone. *J. Clin. Diagn. Res.* 8(6), pp. ZC26–ZC30.

29. Lan J., Wang Z., Wang Y., et al. (2006) The effect of combination of recombinant human bone morphogenetic protein-2and basic fibroblast growth factor or insulin-like growth factor-I on dental implant osseointegration by confocal laser scanning microscopy. *J. Periodontol.* 77(3): 357-363.

30. Laurencin C.T., Ashe K.M., Henry N., et al. (2014) Delivery of small molecules for bone regenerative engineering: preclinical studies and potential clinical applications. *Drug Discov. Today.* 19(6), pp. 794–800.

31. Lee J.H., Kim J., Baek H.-R., et al. (2014) Fabrication of an rhBMP-2 loaded porous β-TCP microsphere-hyaluronic acid-based powder gel composite and evaluation of implant osseointegration. *J. Mater. Sci. Mater Med.* 25(9), pp. 2141–2151.

32. Lee J.K., Choi D.S., Jang I., Choi W.Y. (2015) Improved osseointegration of dental titanium implants by TiO2 nanotube arrays with recombinant human bone morphogenetic protein-2: a pilot in vivo study. *Int. J. Nanomedicine.* 10, pp. 1145-1154.

33. Lee S.W., Hahn B.D., Kang T.Y., et al. (2014) Hydroxyapatite and collagen combination-coated dental implants display better bone formation in the peri-implant area than the same combination plus bone morphogenetic protein-2-coatedimplants, hydroxyapatite only coated implants, and uncoated implants. *J. Oral Maxillofac. Surg.* 72(1), pp. 53-60.

34. Luo T., Zhang W., Shi B., et al. (2012) Enhanced bone regeneration around dental implant with bone morphogenetic protein 2 gene and vascular endothelial growth factor protein delivery. *Clin. Oral Implants Res.* 23(4), pp. 467-473.

35. Ma Q., Wang W., Chu P.K., et al. (2012) Concentration- and time-dependent response of human gingival fibroblasts tofibroblast growth factor 2 immobilized on titanium dental implants. *Int. J. Nanomedicine.* 7, pp. 1965-1976.

36. Mas-Moruno C., Garrido B., Rodriguez D., et al. (2015) Biofunctionalization strategies on tantalum-based materials for osseointegrative applications. *J. Mater. Sci. Mater. Med.* 26(2), pp. 109.

37. Moraschini V., Poubel L.A., Ferreira V.F., Barboza Edos S. (2015) Evaluation of survival and success rates of dental implants reported in longitudinal studies with a follow-up period of at least 10 years: a systematic review. *Int. J. Oral Maxillofac. Surg.* 44(3), pp. 377-388.

38. Mueller C.K., Thorwarth M., Schmidt M., et al. (2011) Comparative analysis of osseointegration of titanium implants with acid-etched surfaces and different biomolecular coatings. *Oral. Surg. Oral. Med. Oral. Pathol. Oral. Radiol. Endodont*. 112(6): 726-736.

39. Mukherjee A., Rotwein P. (2009) Akt promotes BMP2-mediated osteoblast differentiation and bone development. *J. Cell Sci.* 122(Pt 5), pp. 716–726.

40. Muller F., Duvernay E., Loup A., et al. (2013) Implant-supported mandibular overdentures in very old adults: a randomized controlled trial. *J. Dent. Res*. 92(Suppl 2), pp. 154S-160S.

41. Nishimura I. (2013) Genetic networks in osseointegration. *J. Dent. Res*. 92(12 Suppl), pp. 109S–118S.

42. Novochadov V.V., Gayfullin N.M., Zalevskiy D.A., et al. (2013) [The chitosan-coated implants with bioactive surface demonstrate improved characteristics of osseointegration in rats] *[I.P. Pavlov Russian Medical Biological Herald] Rossiyskiy medikobioilogicheskiy vestnik imeni akademika I.P. Pavlova*. (2), pp. 30-35.

43. Ntounis A., Geurs N., Vassilopoulos P., Reddy M. (2015) Clinical assessment of bone quality of human extraction sockets after conversion with growth factors. *Int. J. Oral Maxillofac. Implants*. 2015; 30(1), pp. 196-201.

44. Ogle O.E. (2015) Implant surface material, design, and osseointegration. *Dent. Clin. North Am*. 59(2), pp. 505-520.

45. Ortolani E., Guerriero M., Coli A., et al. A. (2014) Effect of PDGF, IGF-1 and PRP on the implant osseointegration. An histological and immunohistochemical study in rabbits. *Ann. Stomatol. (Roma)*. 5(2), pp. 66-68.

46. Park J.H., Wasilewski C.E., Almodovar N., et al. The responses to surface wettability gradients induced by chitosan nanofilms on microtextured titanium mediated by specific integrin receptors. *Biomater*. 2012; 33(30), pp 7386–7393.

47. Patel Z.S., Young S., Tabata Y., et al. (2008) Dual delivery of an angiogenic and an osteogenic growth factor for bone regeneration in a critical size defect model. *Bone*. 43, pp. 931–940.

48. Petrie T.A., Reyes C.D., Burns K.L., Garcia A.J. (2009) Simple application of fibronectin-mimetic coating enhances osseointegration of titanium implants. *J. Cell Mol. Med.* 13 (8B), pp. 2602-2612.

49. Pye A.D., Lockhart D.E.A., Dawson M.P., et al. (2009) A review of dental implants and infection. *J. Hosp. Infect*. 72(2), pp. 104–110.

50. Russo L., Taraballi F., Lupo C., et al. (2014) Carbonate hydroxyapatite functionalization: a comparative study towards (bio)molecules fixation. *Interface Focus*. 4(1), e20130040.

51. Ryu J.J., Park K., Kim H.S., et al. (2013) Effects of anodized titanium with Arg-Gly-Asp (RGD) peptide immobilized via chemical grafting or physical adsorption on bone cell adhesion and differentiation. *Int. J. Oral Maxillofac. Implants*. 28(4): 963-972.

52. Schliephake H., Aref A., Scharnweber D., et al. (2009) Effect of modifications of dual acid-etched implant surfaces on peri-implant bone formation. Part I: organic coatings. *Clin. Oral Implants Res*. 20(1), pp. 31-37.

53. Schmidlin P.R., Müller P., Attin T., et al. (2013) Polyspecies biofilm formation on implant surfaces with different surface characteristics. *J. Appl. Oral Sci.* 21(1), pp. 48–55.

54. Sumner D.R., Turner T.M., Urban R.M., et al. (2006) Additive enhancement of implant fixation following combined treatment with rhTGF-beta2 and rhBMP-2 in a canine model. *J. Bone Joint Surg. Am*. 88(4): 806-817.

55. Teles F.R., Teles R.P., Uzel N.G., et al. (2012) Early microbial succession in re-developing dental biofilms in periodontal health and disease. *J. Periodontal. Res*. 47(1), pp. 95–104.

56. Tomasi C., Wennström J.L., Berglundh T.J., et al. (2008) Longevity of teeth and implants: a systematic review. *Oral Rehabil*. 35(Suppl. 1), pp. 23-32.

57. Tonetti M., Palmer R., Working Group 2 of the VIII European Workshop on Periodontology (2012) Clinical research in implant dentistry: study design, reporting and outcome measurements. Consensus report of Working Group 2 of the VIII European Workshop on Periodontology. *J. Clin. Periodontol*. 39(Suppl 12), pp. 73-80.

58. Trindade R., Albrektsson T., Wennerberg A. (2015) Current concepts for the biological basis of dental implants: foreign body equilibrium and osseointegration dynamics. *Oral Maxillofac. Surg. Clin. North Am*. 27(2), pp. 175-183.

59. Tsuchiya H., Shirai T., Nishida H., et al. (2012) Innovative antimicrobial coating of titanium implants with iodine. *J. Orthop. Sci.* 17 (5), pp. 595–604.

60. Veitz-Keenan A., Keenan J.R. (2015) Antibiotic use at dental implant placement. *Evid Based Dent.* 2015; 16(2), pp. 50-51.

61. Xuereb M., Camilleri J., Attard N.J. (2015) Systematic review of current dental implant coating materials and novel coating techniques. *Int. J. Prosthodont.* 28(1), pp. 51-59.

62. Yeo I.S. (2014) Reality of dental implant surface modification: a short literature review. *Open Biomed. Eng. J.* 8, pp. 114-119.

63. Yoo D., Tovar N., Jimbo R., et al. (2014) Increased osseointegration effect of bone morphogenetic protein 2 on dental implants: an in vivo study. *J. Biomed. Mater. Res. A.* 102(6), pp. 1921-1927.

64. Zhou L., Lai Y., Huang W., et al. (2015) Biofunctionalization of microgroove titanium surfaces with an antimicrobial peptide to enhance their bactericidal activity and cytocompatibility. *Colloids Surf. B. Biointerfaces.* 128, pp. 552-560.

Примечания:

1. Advances in surfaces and osseointegration in implantology / M. Albertini, M. Fernandez-Yague, P. Lázaro, et al. // Biomimetic surfaces. Med. Oral Patol. Oral Cir. Bucal. – 2015. – Vol. 20, № 3. – e316–e325.

2. Clinical outcomes measures for assessment of longevity in the dental implant literature: ORONet approach. F. Bassi, A.B. Carr, T.L. Chang, et al. // Int. J. Prosthodont. – 2013. – Vol. 26, № 4. – P. 323-330.

3. Berglundh T., Giannobile W.V. Investigational clinical research in implant dentistry: beyond observational and descriptive studies // J. Dent. Res. – 2013. – Vol. 92, Suppl. 12. – P. 107S–108S.

4. Bessa P.C., Casal M., Reis R.L. Bone morphogenetic proteins in tissue engineering: the road from the laboratory to the clinic, part II (BMP delivery) // J. Tissue Eng. Regen. Med. – 2008. – Vol. 2, № 2-3. – P. 81-96.

5. Biological nano-functionalization of titanium-based biomaterial surfaces: a flexible toolbox / R. Beutner, J. Michael, B. Schwenzer, D. Scharnweber // J. Royal Soc. Interface. – 2010. – Vol. 7. – P. S93–S105.

6. Imperforate titanium shell enclosing recombinant human bone morphogenetic protein-2-induced bone formation for high-profile dental implants in rabbit tibia / N. Casap, A. Laviv, M. Debecco, et al. // J. Oral Maxillofac. Surg. – 2015. – Vol. 73, № 2. – P. 245-252.

7. Chang P.-C., Lang N.P., Giannobile W.V. Evaluation of functional dynamics during osseointegration and regeneration associated with oral implants: a review // Clin. Oral Implants Res. – 2010. – Vol. 21, № 1. – P. 1–12.

8. Basic research methods and current trends of dental implant surfaces / P.G. Coelho, J.M. Granjeiro, G.E. Romanos, et al. // J. Biomed. Mater. Res. B. Appl. Biomater. – 2009. – Vol. 88, № 2. – P. 579–596.

9. Silver nanoparticles in dental biomaterials / J.M. Corrêa, M. Mori, H.L. Sanches, et al. // Int. J. Biomater. – 2015. – e485275.

10. The enhancement of bone regeneration by gene activated matrix encoding for platelet derived growth factor / S. Elangovan, D'Mello S.R., Hong L., et al. // Biomaterials. – 2014. – Vol. 35, № 2. – P. 10.

11. Экспериментальная оценка композиционного материала на основе белково-минеральных компонентов и рекомбинантного костного морфогенетического белка (rhBMP-2) в качестве покрытия титановых имплантатов / М.З. Федорова, С.В. Надеждин, А.С. Семихин и др. // Травматология и ортопедия России. – 2011. – № 2,(60). С. 101-106.

12. Osteoinductive peptide-functionalized nanofibers with highly ordered structure as biomimetic scaffolds for bone tissue engineering / X. Gao, X. Zhang, J. Song, et al. // Int. J. Nanomedicine. – 2015. – Vol. 10. – P. 7109–7128.

13. Silver nanoparticle based antibacterial methacrylate hydrogels potential for bone graft applications / M.I. González-Sánchez, S. Perni, G. Tommasi, et al. // Mater. Sci. Eng. C. Mater. Biol. Appl. 2015. – Vol. 50. – P. 332–340.

14. The stability of BMP loaded polyelectrolyte multilayer coatings on titanium . R. Guillot, F. Gilde, P. Becquart, et al. // Biomater. – 2013. – Vol. 34б № 23. – P. 5737–5746.

15. Gupta G. Gingival crevicular fluid as a periodontal diagnostic indicator- I: Host derived enzymes and tissue breakdown products // J. Med. Life. – 2012. – Vol. 5, № 4. – P. 390–397.

16. Harford J. Population ageing and dental care // Com. Dent. Oral Epidemiol. – 2009. – Vol. 37, № 2. – P. 97-103.

17. Recombinant human platelet-derived growth factor: biology and clinical applications / J.O. Hollinger, C.E. Hart, S.N. Hirsch, et al. // J. Bone Joint Surg. Amer. Vol. – 2008. – Vol. 90, Suppl. 1. – P. 48–54.

18. Bio-inspired stable antimicrobial peptide coatings for dental applications / K.V. Holmberg, M. Abdolhosseini, Y. Li, et al. // Acta Biomater. 2013. Vol. 9, № 9. P. 8224–8231.

19. An i*n vitro* assessment of fibroblast and osteoblast response to alendronate-modified titanium and the potential for decreasing fibrous encapsulation / X.Hu, K.G. Neoh, Z. Shi, et al. // Tissue Eng. Pt A. – 2013. – Vol. 19, № 17-18. – P. 1919–1930.

20. Immediately loaded dental implants bioactivated with platelet-rich plasma (PRP) placed in maxillary and mandibular region / F. Inchingolo, A. Ballini, R. Cagiano, et al. // Clin. Ter. – 2015. – Vol. 166, № 3. – P. 146-152.

21. A retrospective study on related factors affecting the survival rate of dental implants / H.W Jang., J.K. Kang, K. Lee, et al. // J. Adv. Prosthodont. – 2011. - Vol. 3, № 4. – P. 204-215.

22. Модификация поверхностей внутрикостных имплантатов: современные исследования и нанотехнологии/ В.И. Калита, Д.А. Маланин, В.А. Мамаева и др. // Вестник Волгоградского гос. мед. ун-та. – 2009. – № 4. – С. 17–22.

23. King W.J., Krebsbach P.H. Growth factor delivery: How surface interactions modulate release in vitro and in vivo // Adv. Drug Deliv. Rev. – 2012. – Vol. 64, № 12. – P. 1239–1256.

24. Effect of local sequential VEGF and BMP-2 delivery on ectopic and orthotopic bone regeneration / D.H.Kempen, L. Lu, A. Heijink, et al. // Biomater. – 2009. – Vol. 30. – Vol. 2816–2825.

25. Periodontal tissue regeneration using fibroblast growth factor-2: randomized controlled phase II clinical trial / M. Kitamura, K. Nakashima, Y. Kowashi, et al. // PLoS ONE. – 2008. – e2611.

26. Substituted hydroxyapatites with antibacterial properties / J. Kolmas, E. Groszyk, D. Kwiatkowska-Różycka // Biomed. Res. Int. – 2014. – e178123.

27. Erk pathways negatively regulate matrix mineralization / S.J. Kono, Y. Oshima, K. Hoshi, et al. // Bone. – 2007. – Vol. 40, № 1. – P. 68–74.

28. Kundu R., Rathee M. Effect of platelet-rich-plasma (PRP) and implant surface topography on implant stability and bone // J. Clin. Diagn. Res. – 2014. – Vol. 8, № 6. – P. ZC26–ZC30.

29. The effect of combination of recombinant human bone morphogenetic protein-2and basic fibroblast growth factor or insulin-like growth factor-I on dental implant osseointegration by confocal laser scanning microscopy / J. Lan, Z. Wang, Wang Y., et al. // J. Periodontol. – 2006. – Vol. 77, № 3. – P. 357-363.

30. Delivery of small molecules for bone regenerative engineering: preclinical studies and potential clinical applications / C.T. Laurencin, K.M. Ashe, N. Henry, et al. // Drug Discov. Today. – 2014. – Vol. 19, № 6. – P. 794–800.

31. Fabrication of an rhBMP-2 loaded porous β-TCP microsphere-hyaluronic acid-based powder gel composite and evaluation of implant osseointegration / J.H. Lee, J. Kim, H.-R. Baek, et al. // J. Mater. Sci. Mater Med. – 2014. – Vol. 25, № 9. – P. 2141–2151.

32. Improved osseointegration of dental titanium implants by TiO2 nanotube arrays with recombinant human bone morphogenetic protein-2: a pilot in vivo study / J.K. Lee, D.S. Choi, I. Jang, W.Y. Choi // Int. J. Nanomedicine. – 2015. – Vol. 10. – P. 1145-1154.

33. Hydroxyapatite and collagen combination-coated dental implants display better bone formation in the peri-implant area than the same combination plus bone morphogenetic protein-2-coatedimplants, hydroxyapatite only coated implants, and uncoated implants / S.W. Lee, B.D. Hahn, T.Y. Kang, et al. // J. Oral Maxillofac. Surg. – 2014. – Vol. 72, № 1. – P. 53-60.

34. Enhanced bone regeneration around dental implant with bone morphogenetic protein 2 gene and vascular endothelial growth factor protein delivery / T. Luo, W. Zhang, B. Shi, et al. // Clin. Oral Implants Res. – 2012. – Vol. 23, № 4. – P. 467-473.

35. Concentration- and time-dependent response of human gingival fibroblasts to fibroblast growth factor 2 immobilized on titanium dental implants / Q. Ma, W. Wang, P.K. Chu, et al. // Int. J. Nanomedicine. – 2012. – Vol. 7. – P. 1965-1976.

36. Biofunctionalization strategies on tantalum-based materials for osseointegrative applications / C. Mas-Moruno, B. Garrido, D. Rodriguez, et al. // J. Mater. Sci. Mater. Med. – 2015. – Vol. 26, № 2. - P. 109.

37. Evaluation of survival and success rates of dental implants reported in longitudinal studies with a follow-up period of at least 10 years: a systematic review / V. Moraschini, L.A. Poubel, V.F. Ferreira, S. Barboza Edos // Int. J. Oral Maxillofac. Surg. – 2015. – Vol. 44, № 3. – P. 377-388.

38. Comparative analysis of osseointegration of titanium implants with acid-etched surfaces and different biomolecular coatings / C.K. Mueller, M. Thorwarth, M. Schmidt, et al. // Oral. Surg. Oral. Med. Oral. Pathol. Oral. Radiol. Endod. – 2011. – Vol. 112, № 6. – P. 726-736.

39. Mukherjee A., Rotwein P. Akt promotes BMP2-mediated osteoblast differentiation and bone development // J. Cell Sci. – 2009. – Vol. 122, Pt. 5. – P. 716–726.

40. Implant-supported mandibular overdentures in very old adults: a randomized controlled trial / F. Muller, E. Duvernay, A. Loup, et al. // J. Dent. Res. – 2013. – Vol. 92, Suppl 2. – P. 154S-160S.

41. Nishimura I. Genetic networks in osseointegration // J. Dent. Res. – 2013. – Vol. 92, Suppl 12. – P. 109S–118S.

42. Остеоинтеграция имплантатов с биоактивной поверхностью, модифицированной напылением хитозана в эксперименте у крыс / В.В. Новочадов, Н.М. Гайфуллин, Д.А. Залевский и др. // Российский медико-биологический вестник им. академика И.П. Павлова. – 2013. – № 2. – С. 30-35.

43. Clinical assessment of bone quality of human extraction sockets after conversion with growth factors / A. Ntounis, N. Geurs, P. Vassilopoulos, M. Reddy // Int. J. Oral Maxillofac. Implants. – 2015. – Vol. 30, № 1. – P. 196-201.

44. Ogle O.E. Implant surface material, design, and osseointegration // Dent. Clin. North Am. – 2015. – Vol. 59, № 2. – P. 505-520.

45. Effect of PDGF, IGF-1 and PRP on the implant osseointegration. An histological and immunohistochemical study in rabbits / E. Ortolani, M. Guerriero, A. Coli, et al. // Ann. Stomatol. (Roma). – 2014. – Vol. 5, № 2. – P. 66-68.

46. The responses to surface wettability gradients induced by chitosan nanofilms on microtextured titanium mediated by specific integrin receptors/ J.H. Park, C.E. Wasilewski, N. Almodovar, et al. // Biomaterials. – 2012. – Vol. 33, № 30. – P. 7386–7393.

47. Dual delivery of an angiogenic and an osteogenic growth factor for bone regeneration in a critical size defect model / Z.S. Patel, S. Young, Y. Tabata, et al. // Bone. – 2008. – Vol. 43. – P. 931–940.

48. Simple application of fibronectin-mimetic coating enhances osseointegration of titanium implants / T.A. Petrie, C.D. Reyes, K.L. Burns, A.J. Garcia // J. Cell Mol. Med. – 2009. – Vol. 13, № 8B. – P. 2602-2612.

49. A review of dental implants and infection / A.D. Pye, D.E.A. Lockhart, M.P. Dawson, et al. // J. Hosp. Infect. – 2009. – Vol. 72, № 2. – P. 104–110.

50. Carbonate hydroxyapatite functionalization: a comparative study towards (bio)molecules fixation / L. Russo, F. Taraballi, C. Lupo, et al. // Interface Focus. – 2014. – Vol. 4, № 1. – e20130040.

51. Effects of anodized titanium with Arg-Gly-Asp (RGD) peptide immobilized via chemical grafting or physical adsorption on bone cell adhesion and differentiation / J.J. Ryu, K. Park, H.S. Kim, et al. // Int. J. Oral Maxillofac. Implants. – 2013. – Vol. 28, № 4. – P. 963-972.

52. Effect of modifications of dual acid-etched implant surfaces on peri-implant bone formation. Part I: organic coatings / H. Schliephake, A. Aref, D. Scharnweber, et al. // Clin. Oral Implants Res. – 2009. – Vol. 20, № 1. – P. 31-37.

53. Polyspecies biofilm formation on implant surfaces with different surface characteristics / P.R. Schmidlin, P. Müller, T. Attin, et al. // J. Appl. Oral Sci. – 2013. – Vol. 21, № 1. – P. 48–55.

54. Additive enhancement of implant fixation following combined treatment with rhTGF-beta2 and rhBMP-2 in a canine model / D.R. Sumner, T.M. Turner, R.M. Urban, et al. // J. Bone Joint Surg. Am. – 2006. – Vol. 88, № 4. – P. 806-817.

55. Early microbial succession in re-developing dental biofilms in periodontal health and disease / F.R. Teles, R.P. Teles, N.G. Uzel, et al. // J. Periodontal. Res. 2012. – Vol. 47, № 1. – P. 95–104.

56. Tomasi C., Wennström J.L., Berglundh T.J. Longevity of teeth and implants: a systematic review // Oral Rehabil. – 2008. – Vol. 35, Suppl. 1. – P. 23-32.

57. Clinical research in implant dentistry: study design, reporting and outcome measurements. Consensus report of Working Group 2 of the VIII European Workshop on Periodontology. / M. Tonetti, R. Palmer, Working Group 2 of the VIII European Workshop on Periodontology // J. Clin. Periodontol. – 2012. – Vol. 39, Suppl 12. – P. 73-80.

58. Trindade R., Albrektsson T., Wennerberg A. Current concepts for the biological basis of dental implants: foreign body equilibrium and osseointegration dynamics // Oral Maxillofac. Surg. Clin. North Am. – 2 15. – Vol. 27, № 2. – P. 175-183.

59. Innovative antimicrobial coating of titanium implants with iodine / H. Tsuchiya, T. Shirai, H. Nishida, et al. // J. Orthop. Sci. – 2012. - Vol. 17, № 5. – P. 595–604.

60. Veitz-Keenan A., Keenan J.R. Antibiotic use at dental implant placement // Evid. Based Dent. – 2015. – Vol. 16, № 2. – P. 50-51.

61. Xuereb M., Camilleri J., Attard N.J. Systematic review of current dental implant coating materials and novel coating techniques // Int. J. Prosthodont. – 2015. – Vol. 28, № 1. – P. 51-59.

62. Yeo I.S. Reality of dental implant surface modification: a short literature review. // Open Biomed. Eng. J. – 2014. – Vol. 8. – P. 114-119.

63. Increased osseointegration effect of bone morphogenetic protein 2 on dental implants: an in vivo study / D. Yoo, N. Tovar, R. Jimbo, et al. // J. Biomed. Mater. Res. A. – 2014. – Vol. 102, № 6. – P. 1921-1927.

64. Biofunctionalization of microgroove titanium surfaces with an antimicrobial peptide to enhance their bactericidal activity and cytocompatibility / L. Zhou, Y. Lai, W. Huang, et al. // Colloids Surf. B. Biointerfaces. 2015; 128: 552-560.

УДК 57.089.67 : 616.314-089

Молекулярные технологии функционализации поверхности дентальных имплантатов

Ангелина Олеговна Зекий

Первый Московский медицинский университет, Российская Федерация
119991, г. Москва, ул. Трубецкая, 8, стр. 2
Кандидат медицинских наук, доцент
E-mail: angelinaolegovna@gmail.com

Аннотация. Настоящий обзор рассматривает несколько подходов к улучшению свойств дентальных имплантатов за счет модификации их биоактивной поверхности (функционализации) с помощью технологий молекулярной трансплантации. Первая группа функциональных лигандов призвана усилить остеоинтеграцию имплантатов, и представлена факторами роста, способствующими образованию и ремоделированию костной ткани: костными морфогенетическими белками (BMPs), тромбоцитарным фактором роста (PDGF), фактором роста фибробластов (FGF), а также их комбинациями между собой и с рядом других факторов роста. Вторая группа биоактивных молекул напрямую не стимулирует образование костной ткани, но за счет стимуляции адгезии, способствует укоренению остеобластов на поверхности имплантата, тем самым уменьшая сроки наступления остеоинтеграции. Наконец, третья группа веществ используется для

увеличения антибактериальных свойств покрытий, способствует уменьшению образования бактериальных пленок на поверхности имплантата, снижает риск развития его воспалительного отторжения. Ключевые проблемы использования биофункциональных покрытий, несмотря на их явную перспективность, на сегодня по-прежнему состоят в относительной дороговизне, трудности контролирования свойств и их сохранения в период между изготовлением и установкой имплантатов в кость реципиента.

Ключевые слова: дентальная имплантация, функциональные покрытия, биоактивная поверхность, клеточная адгезия, остеоинтеграция, тромбоцитарный фактор роста, костные морфогенетические белки.